Tectonic imprints of landscape evolution in the Bhilangana and Mandakini basin, Garhwal Himalaya, India: A geospatial approach

Ajay Kumar Taloor [a,*], Lalit Mohan Joshi [b], Bahadur Singh Kotlia [b], Akhtar Alam [c,g], Girish Ch Kothyari [d], Raj Sunil Kandregula [d], Anoop Kumar Singh [e], Rakesh Kumar Dumka [d]

[a] *Department of Remote Sensing and GIS, University of Jammu, Jammu, 180006, India*
[b] *Centre of Advanced Study in Geology, Kumaun University, Nainital, 263001, India*
[c] *Department of Geography & Regional Development, University of Kashmir, Srinagar, 190006, India;*
[d] *Institute of Seismological Research Gandhinagar, Gujarat, India*
[e] *Department of Geology, Lucknow University, Lucknow, 226007, India*
gUCL Institute for Risk and Disaster Reduction, London, UK

ARTICLEINFO

Keywords:
Landscape evolution
Morphotectonic analysis
Tectonic imprints Garhwal
himalaya

ABSTRACT

Torrential rains, landslides, and seismic activity are the common factors that are causing unprecedented damage to life, property and infrastructure in Mandakini and Bhilangana basins of Garhwal Himalaya. Owing to such conditions, we demonstrate the feedback this landscape in Garhwal Himalaya in response to episodic tectonic uplift and monsoon precipitation. We calculated conventional geomorphic parameters to access the tectonic deformation across the major thrusts and faults. We further analyzed the normalized steepness index (K_{sn}), Chi (χ), and knickpoints along the longitudinal course of rivers. Additionally, the study attributed to active nature of Chail/Ramgarh thrust along the Balganga valley as envisaged by five levels of unpaired fluvial terraces, entrenched stream course, river ponding, active and stabilized landslide deposits, etc. Moreover, the flooding during the heavy rainfall events induced river toe cutting makes an effect on settlement over fluvial deposits. Therefore, we suggested that the highly dissected and tilted basins with deep V shaped valleys and ongoing seismicity also fabricates the region more vulnerable for hazards which threaten the human lives.

1. Introduction

The drainage pattern of the river systems is highly sensitive to tectonically driven changes and are able to preserve the records of for- mation and progression of most tectono-geomorphic processes that occur within its confines (Phartiyal and Kothyari, 2012; Dubey et al., 2017; Xue et al., 2018; Alam et al., 2018; Sarkar et al., 2020). Hence, the landform evolution is the consequences of the evolution of individual drainage basins of which it is created (Singh and Gupta, 1980; Khan et al., 2020). The morphotectonic analyses is significant in under- standing the fluvial geomorphic processes, tectonic influence of land- scape and their role to drainage development (Horton, 1945; Schumm, 1956; Bull and McFadden, 1977; Keller and Pinter, 1996). Globally, the Digital Elevation data is used as an essential tool in GIS environment to analyze the morphotectonic characteristics of the drainage basins (Montgomery and Foufoula-Georgiou, 1993; Tucker, 1996; Hajam et al., 2013; Kothyari, 2014; Kothyari et al., 2016a, 2017a, 2016b; Waikar and Nilawar, 2014; Sklar and Dietrich, 1998; Weissel and Seidl, 1998; Singh et al., 2017, 2020; Sood et al., 2020). Conventionally, the drainage systems in an active tectonic terrain is impacted by river incisions, active folding and faulting and erodibility which leads to the formation of several alluvial landforms (Schumm, 1986; Keller and Pinter, 1996; Whipple et al., 2013; Kothyari, 2014; Kothyari et al., 2016a, 2018a; Taloor et al., 2017). Active tectonics induced deformation of the valley floor can affect the geometry, aggradation and degradation process of the fluvial network and the deformation can be observed in the form of streams/terrace offsets along the faults (Wallace and Moxham, 1967; Kothyari and Luirei, 2016; Kothyari et al., 2017b, 2020b, 2018b; Bhat et al., 2019). Factors such as topography, climate and lithological con- trol also effects the geomorphic processes which must be considered while inferring from a tectonically oriented aspect (Jackson and Leeder, 1994; Holbrook and Schumm, 1999; Burbank and Anderson, 2001; Keller and Pinter, 2002). Evaluating tectonic deformation rates using chronological studies, geomorphologic, geologic and meteorological data are the conventionally adopted aspects to characterize the nature of active faults (Molin et al., 2004; Dumont et al., 2005; Necea et al., 2005;

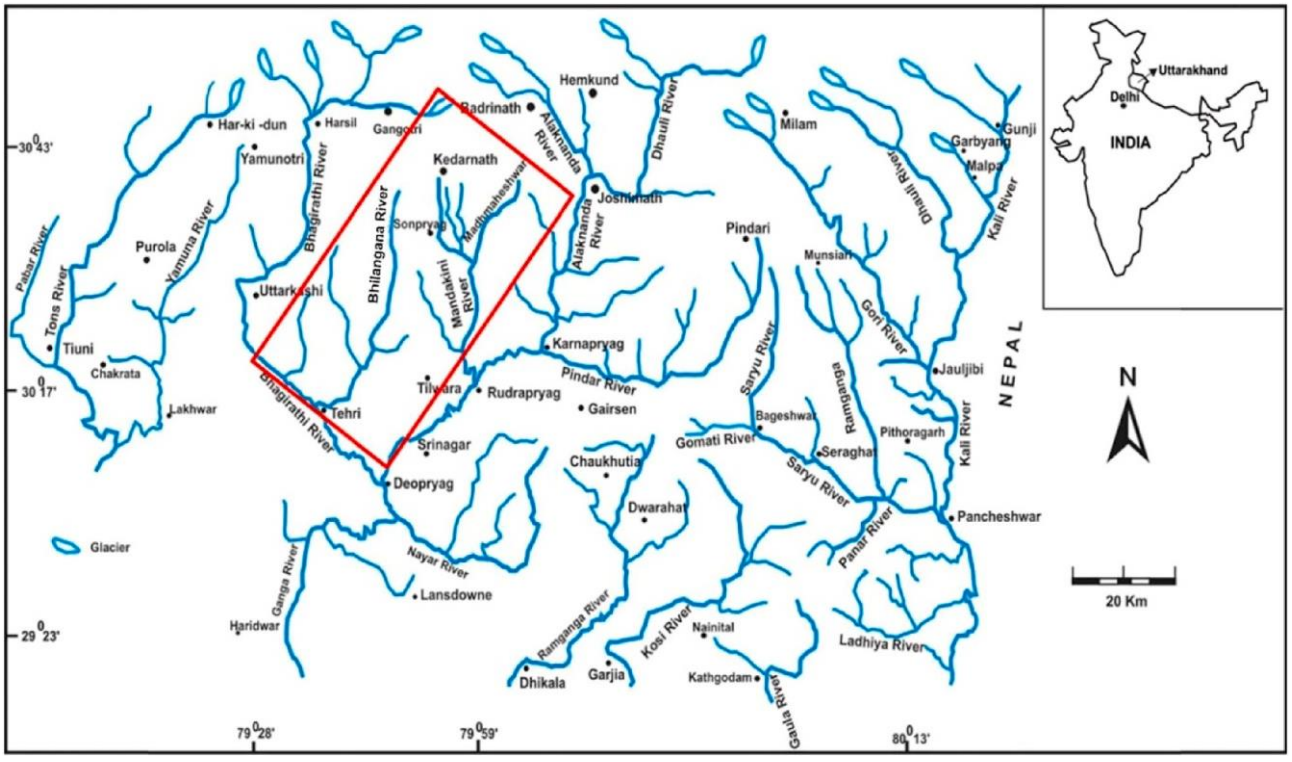

Fig. 1. Major river's networks in Uttarakhand Himalaya along with studied Bhilangana basin upper catchment of Ganga River (after Valdiya, 1980).

Giaconia et al., 2012; Alam et al., 2017; Knight and Grab, 2018; Taloor et al., 2019; Kumar et al., 2020; Haque et al., 2020). Not only tectonic driven uplift but also subordinate climatic fluctuations produces erosional landforms and other geomorphic processes such as channel incision, river deflection, river piracy, headworderosion, etc. (Holbrook and Schumm, 1999; Snyder et al., 2000; Burbank and Anderson, 2001; Lave and Avouac, 2001; Hilley and Arrowsmith, 2008; Asthana et al., 2018; Kothyari et al., 2019).

The topographic building of the Himalaya is a consequence of the external (climatic) and internal dynamic (tectonics) interactions in the Indian plate which is subducting beneath the Eurasian plate after collision (Quereshy et al., 1989; Juyal et al., 2010; Ray and Srivastava, 2010; Kannaujiya et al., 2020). The river valleys proximal to thrusts/- faults within the Himalayas provide ample geomorphic evidences of tectonic activity. Therefore, in the present study we investigated Bhilangana and Mandakini river basins which are bounded by Main Central Thrust (MCT) in the north and Main Boundary Thrust (MBT) in the south to understand the landform modifications caused by tectonic activity and erosional processes. The geomorphic record in the mountains and in their forelands reflects the interplay of orogenic tectonics, global cli- matic changes and therefore, provides a unique opportunity to under- stand realm of neotectonics. The deflection of river channels in the (which part upper lower) Himalayas can be straightaway correlated with neoteconic activity prevailing in the region which effects river gradient and generates knickpoints (Gupta, 1997; Seeber and Gornitz, 1983; Kothyari and Luirei, 2016; Talukdar et al., 2019; Kothyari et al., 2020b). Active fault zones present in the Higher Himalaya can be detected by observing abrupt changes in river gradient and the gradient is maximum towards north and it gets moderate approaching south indicating rapid uplift activity in the former part which coincides with regions of rapid uplift in the north to moderate uplift in the south (Hodges et al., 2004).

In the recent years, natural disasters have claimed many lives and caused large scale property damage throughout the Himalaya region exclusively in the areas experiencing neotectonic movements added by unplanned constructions and settlements on fluvial and unconsolidated sediments in various regions. Besides this, the Garhwal Himalaya is subjected to heavy rainfall every year that caused swiftness of disasters under fragile lithology. Due to high relief and dense vegetation condi- tions, some parts in Himalayan region are inaccessible to conduct geological/geomorphic investigations to assess its tectonic history. Therefore, the remote sensing (RS) and geographic information systems (GIS) techniques proved to be an indispensable tool in evaluating mor- photectonic analysis to estimate tectonic activity (Taloor et al., 2017; Kothyari et al., 2020b).

In this paper, we have carried out morphotectonic analysis based on GIS in the Bhilangana and Mandakini basins of the Garhwal Himalaya, India. These basins are part of the upper catchment of Bhagirathi River, later called the Ganga River after meeting with the Alaknanda River at Devprayag, which is an ecologically sensitive area. The morphotectonic study can quantify the characteristic of river drainage and its development in the tectonically active regions because it has a close control of interplay between tectonics and climate (Rockwell et al., 1984; Bull and Knuepfer, 1987; Keller and Pinter, 1996).

2. Physiography and climate of the study area

The Bhilangana and Mandakini river basins in the Garhwal Hima- laya, Uttarakhand are bounded by 30° 20^0 to 30° 52^0 N latitudes and 78°28^0 to 79° 22^0 E longitudes (Fig. 1). The basins have a catastrophic his- tory of rainfall induced mass movements, debris flows and snow ava- lanches. The high relief of the study area with a variation in elevation from 378 to 7000 m is also responsible for instability in the area. The extreme climatic fluctuations with limited economic resources causes harsh living conditions in the study area. Approximately 80% of the annual rainfall in the study area is received from June to September from the Indian Summer Monsoon (ISM). High altitude mountains act as a barrier creating fluctuations in thermal pressure leading to conden- sation of huge cloud masses causing cloud bursts and converting them into torrential rains. The westerlies also play a significant role and

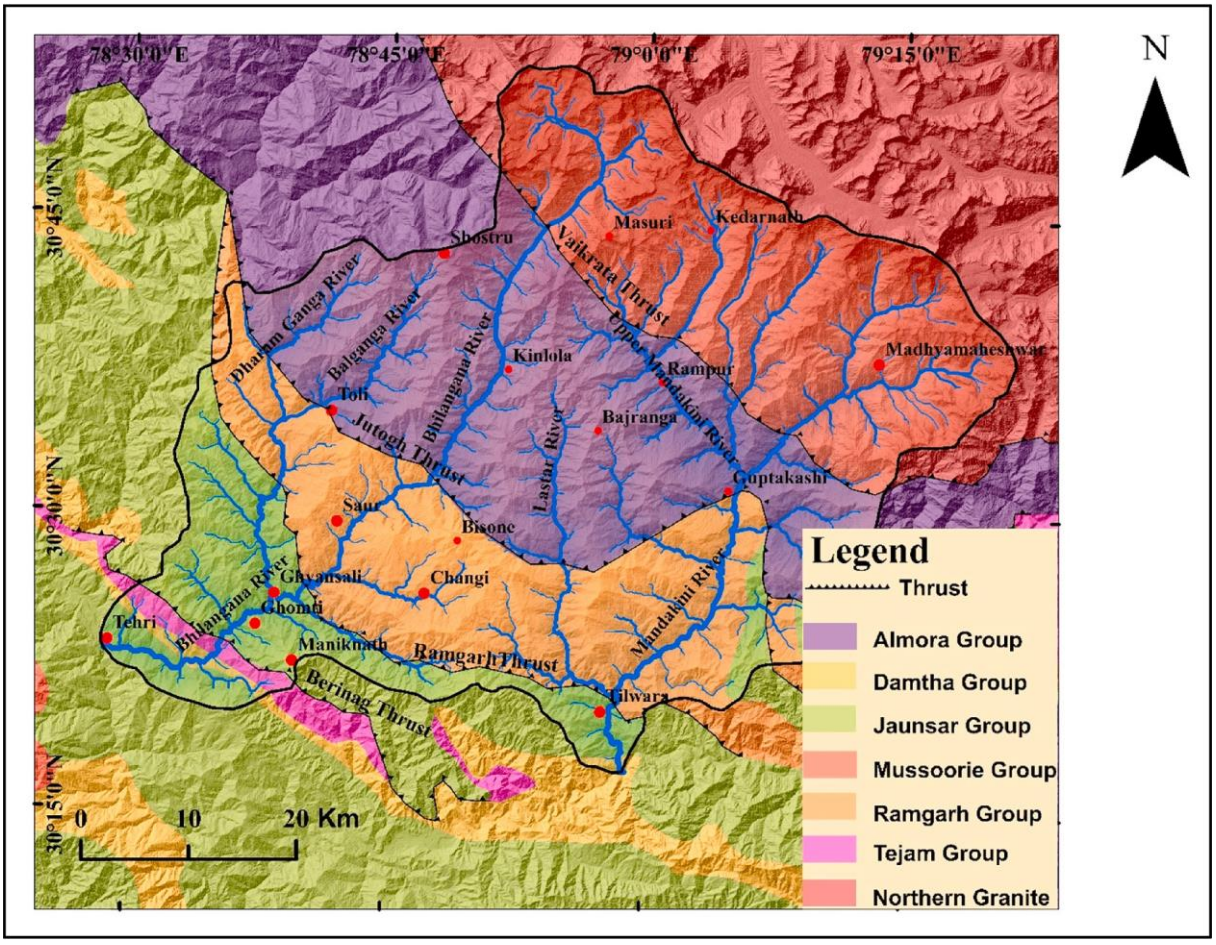

Fig. 2. Geology map of the study area (after, Valdia, 1980).

contribute about 20% of annual precipitation (Kumar et al., 2020).

2.1. Geology and tectonic set-up

Litho-tectonically, the Himalaya is subdivided into four roughly parallel mountain ranges such as Trans Himalaya, Higher Himalaya, Lesser Himalaya and Sub-Himalaya (Le-Fort, 1996; Godin, 2003; Yeats and Thakur, 2008), which are separated from each other by the intra-crustal boundaries (thrust/faults) such as Trans Himadri Fault (THF), Main Central Thrust (MCT), Main Boundary Thrust (MBT) and Himalayan Frontal Fault (HFF) from North to south respectively (Valdiya, 1980). The present study area falls in the Garhwal Himalaya which lies near the central part of the Himalayan belt and is, therefore, a critical area for studying the typical characteristics of the Himalayan fold-and-thrust belt (Srivastava and Mitra, 1994). The Lesser Himalaya in Kumaun-Garhwal region is structurally the lowest slice (Yin and Harrison, 2000). It is bounded by the MCT and MBT in North and south respectively, and generally made-up by clastic sediments and meta sedimentary rocks of Precambrian ages (Brookfield, 1993; Yin and Harrison, 2000; Yin, 2006). The area is mostly built up by three nappes (e.g., the sedimentary Krol Nappe (Berinag Formation), the epi-metamorphic Ramgarh (Chail) Nappe, and the mesometamorphic Almora (Jutogh) Nappe) overriding the autochthonous of Damtha and Tejam Group (Valdiya, 1981). The lesser Himalayan sequence is over- lain by rocks of Vaikrita group along the MCT.

The present study area is made up with the rocks of Ramgarh, Jutogh/Almora and Vaikrita Groups along the Bhilangana and Man- dakini valleys (Fig. 2). The biotite-quartz-albite microcline tourmaline bearing geniss is pelitic and is characterized by intercalations of quartzo-feldspathic schist are observed along the Bhilangana valley (Saklani, 1993). Saklani and Bahuhuna (1983) studied the granite gneiss (Bud- hakedar) and its tectonic disposition along the Balganga-Bhilangana valleys and remarked that MCT zone (III) consisted of streaky gneiss, granite gneiss and mylonite gneiss. The MCT in the crystalline nappe zone is constituted by the high grade Vaikrita (I), medium grade Jutogh (II) and low grade Budhakedar (III) planes, The MCT-I (Varikrita) was split into MCT-II (Jutogh) along Mandakini and Bhagirathi valleys. Further, the Bhilangana Duplex is defined by the MCT-I and MCT-III (Bhudakedar) and consisting of MCT-III and Jutogh Klippen (Bahu- guna and Saklani, 1988). Thus, the MCT-I, II and II, the crystallines and metamorphic of the Bhilangana duplex have undergone shortening (Saklani, 1993). Further, the Mandakini duplex consisting of Jutogh Klippen (upper-Guptakashi duplex) and Budhakedar nappe (lower-Kund duplex) is characterized by MCT-I, II and III (Saklani, 1993). The thrust sheets of Garhwal Himalaya are northerly dipping lateral sequences, orogenically falling in the Lesser Himalaya (LH) (Kumar et al., 2012). Further, radon, based study along these thrusts in Gahrwal Himalaya shows the imbricate nature of the Chail Thrust near Budhakedar and Chamiyala region (Choubey and. Ramola, 1997). The study also reveals that the higher radon concentration in soil, air and groundwater in the Bhilangana Valley because of the presence of thrusts, faults and shear within the region.

3. Method and material

In the present study, our main aim is to quantify the neotectonic activity prevailing in the region by using multidisciplinary approach using geology, geomorphology, morphotectonic and rainfall anomaly.

Table 1
Morphometric parameters used in the present study.

S. No.	Indices	Formula	Variables	References
1	Stream length Gradient Index (SL)	SL ¼ (ΔH/ ΔL) L	ΔH/ΔL ¼ channel slope or gradient of the reach ΔH ¼ is the change in elevation ΔL ¼ is the length of the reach L ¼ is the total channel length from the point of interest	Hack (1973) Bull (2009)
2	Asymmetry Factor (AF)	AF ¼ 100 (Ar/At)	Ar is the area of the basin to the right (facing downstream) of the trunk stream and At is the total area of the drainage basin.	Keller and Pinter (2002)
3	Transverse Topographic Symmetry Factor (T)	T ¼ Da/Dd	Da is the distance from the midline of the drainage basin to the midline of the active meander belt, and Dd is the distance from the basin midline to the basin divide.	Horton (1945)
4	Valley Floor Width to Valley Height (Vf)	(Vf) ¼ 2Vfw/ [(Eld-Esc)/ (Erd-Esc)]	Where Vfw ¼ width of the valley floor, Eld and Erd ¼ elevations of left and right valley divides and Esc ¼ elevation of the valley	Keller and Pinter (2002)
5	Hypsometric curve	HI $H_{mean} = H_{min}/H_{max} - H_{min}$	H_{mean}, H_{max}, and H_{min} are the mean, maximum, and minimum elevation	Strahler (1952); Schumm (1956)
6	Steepness Index (Ks)	$S = Ks\,A^{-\theta}$	S ¼ local channel slope A ¼ is the stream drainage area Ks ¼ is the steepness index Θ ¼ is the concavity	Goldrick and Bishop (2007) Whipple et al. (2013)

Table 2

Morphotectonic parameters in different sub basins and its lithological associations.

Name and notations of subbasins	Morphotectonic parameters				
	Af (Af50)	HI	Vf	T	SL
I Balganga	67 (17) Asymmetric	0.39 Concave	0.42	0.45	354
II Chinkyana	64 (14) Moderately symmetric	Complex 0.60	0.59	0.61	2371
III Bhilangana	44 (6) Slightly symmetric	0.42 Concave	0.83	0.78	389
IV Upper Mandakini	48 (2) Symmetric	0.76 Convex	0.33	0.29	880
V Mukteshwar Ganga	77 (27) Asymmetric	0.65Convex	0.27	0.33	1532
VI Lastar	30 (20) Asymmetric	0.58 Convex	0.63	0.57	367
VII Mandakini	49 (1) Symmetric	Complex 0.62	0.72	0.82	320

(HC) and Hypsometric Integral (HI). For evaluation of these parameters we have used Survey of India (SOI) topo sheets Nos. 53O/13 and 53C/2;

at 1:50,000 scale and ALOS PALSAR Digital Elevation Model (DEM) of 12.5 m resolution. Further, we have prepared slope and aspect map for

the study area to determine the slope percentage and aspect direction using the DEM. We identified several zones of deformation from the satellite data and carried out detailed field investigation to assess the neotectonic activity in the region. The monthly mean precipitation and temperature data of both basins were taken from Indian water portal (IWP) (http://www.waterportal). The Himalayan region has experi- enced a large number of high, moderate and low magnitude earthquakes

in the present and past century and it is suggested that the entire Uttarakhand Himalaya is seismically active. To study the past seismic

events and its impact on the landscape and tectonics of the area the data from USGS seismic data were used (http://earthquake.usgs.gov/earth quake.s/).

The details of each morphometric parameter evaluated is given in Table 1. Furthermore, for the estimation of Chiχ and Knickpoint analysis we adopted similar methodology as used by Kothyari et al. (2020a).

3.1. Morphometric parameters

3.1.1. Asymmetric factor (Af)

The formula for evaluating the Af is given in Table-1. If the value of

the Af is greater than or less than 50, it implies that the basin is asym- metric in nature and is believed to be developed under active tectonic regime or due to the strong lithologic control. If the Af value is greater than 50 it indicates that the basin is tilting towards left facing down- stream (Pinter and Keller, 2002). The values shown in Table 2 for Af

includes the amount of difference between the neutral value of 50 and

the observed value i.e. Af-50.

5.1.1. Stream-length gradient index (SL)

SL can be calculated by the formula mentioned in Table-1. The SL

index is calculated from the upper reaches of the channel (Merrits and Vincent, 1989). Unusual values of the SL along the channel indicate it is affected by rock resistance/increase or decrease in stream power or due to tectonic activity.

6.1.1. Transverse topographic symmetry factor (T)

Transverse topographic symmetry factor assumes that the dip di- rection of the bedrock has little or no influence in migrating stream

channels. This indicates that the regional migration and ground tilting are happening in the same direction (Horton, 1945; Keller and Pinter, 2002). Therefore, T has both direction and magnitude from 0 to 1. If the basin is symmetrical then the value of T equals 0 and the asymmetry increases the value of T increases and reaches a maximum of 1.

6.1.2. Valley floor width to valley height ratio (Vf)

The valley floor width to valley height ratio differentiates between broad canyons and narrow valleys, where the broad floor canyons pro- duce high values of Vf and the narrow valleys contribute low Vf values.
The relatively high values of Vf indicate that the streams have carved

broad valley floors attributed to low uplift rates, while low values of Vf that reflect deep valleys with streams that are actively incising (Keller

and Pinter, 2002).

6.1.3. Hypsometric curve and integral (HC and HI)

We have calculated various geomorphic parameters that help in assessing the tectonic activity in the region i.e. Asymmetric factor (Af), Stream length gradient index (SL), Transverse topographic symmetry factor (T), Valley floor width to height ratio (Vf), Hypsometric Curve

The hypsometric curve and hypsometric integral (HI) are helpful in determining the developmental stages of the drainage basin (Strahler, 1952). The hypsometric curve indicates degree of dissection of the basin,

i.e., erosional stage of the basin. Concave profiles represent long-term equilibrium between uplift and erosion rates. Concave–convex profiles with erosion steps in the middle reaches indicate long-term predomi- nance of erosional processes. Convex profiles are characteristic of areas

where uplift (active tectonics) is dominant (Men□ndez et al., 2008). The

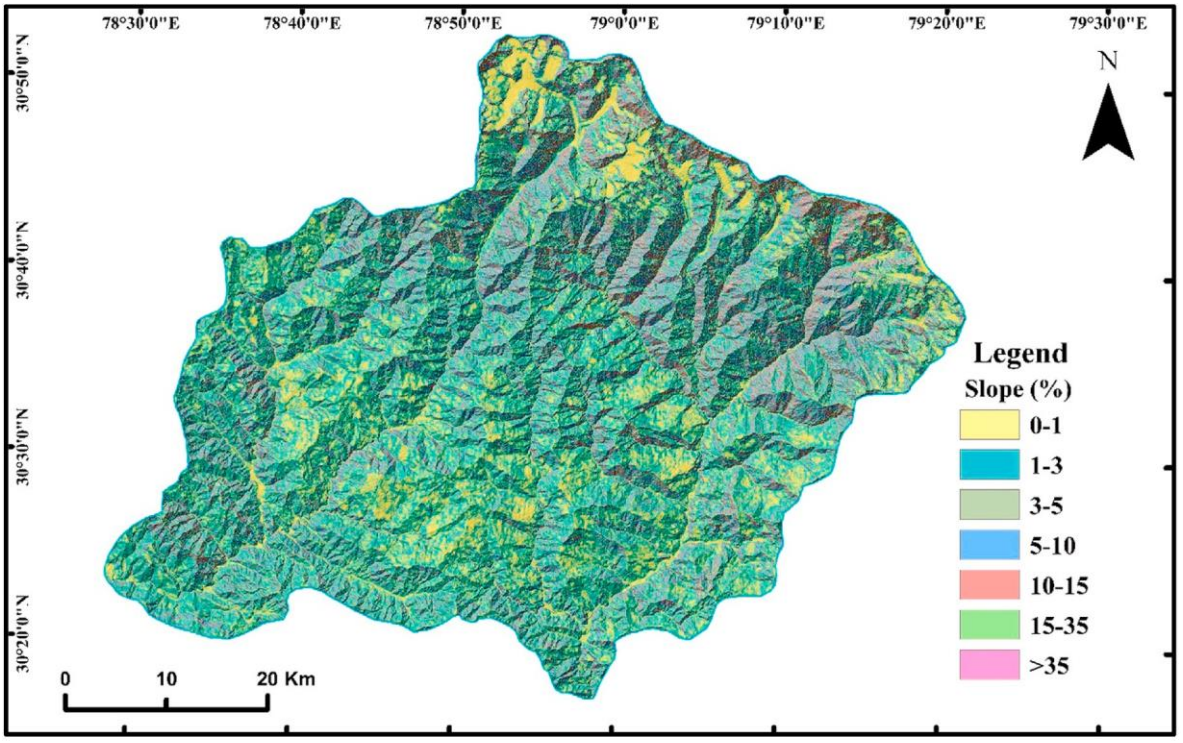

3a Slope map of the study area.

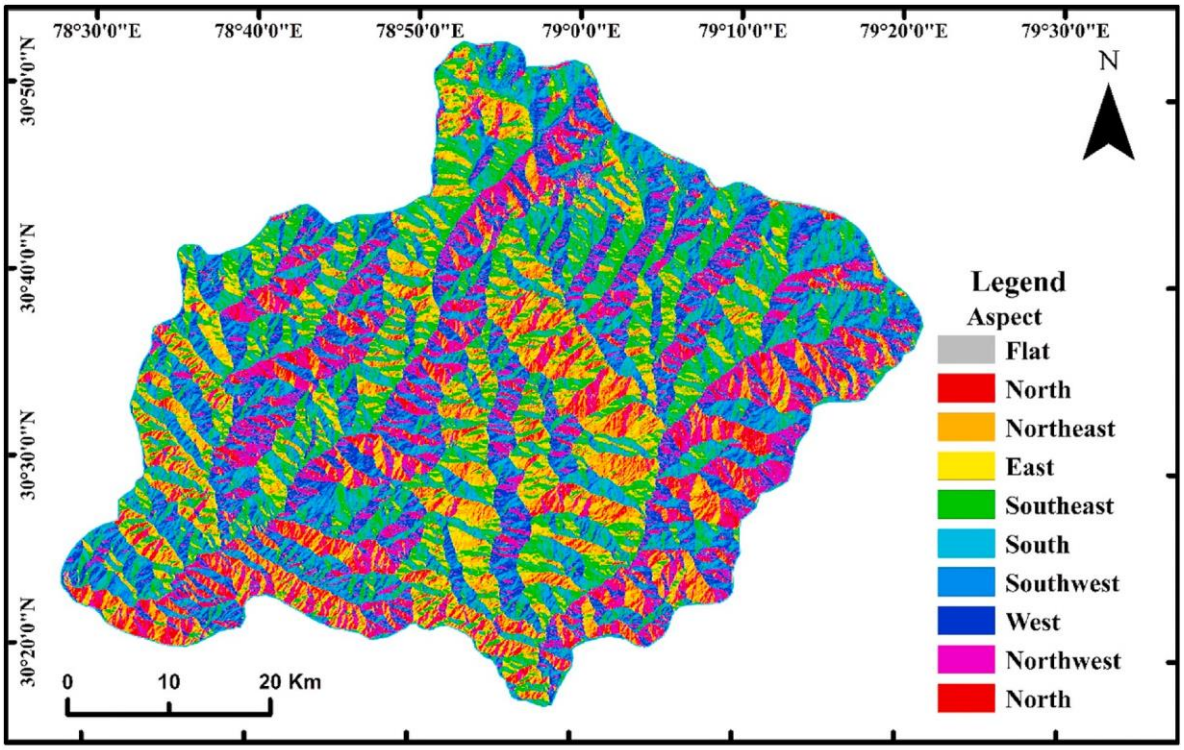

3b Aspect map of the study area.

Fig. 3. a Slope map of the study area.
Fig. 3bAspect map of the study area.

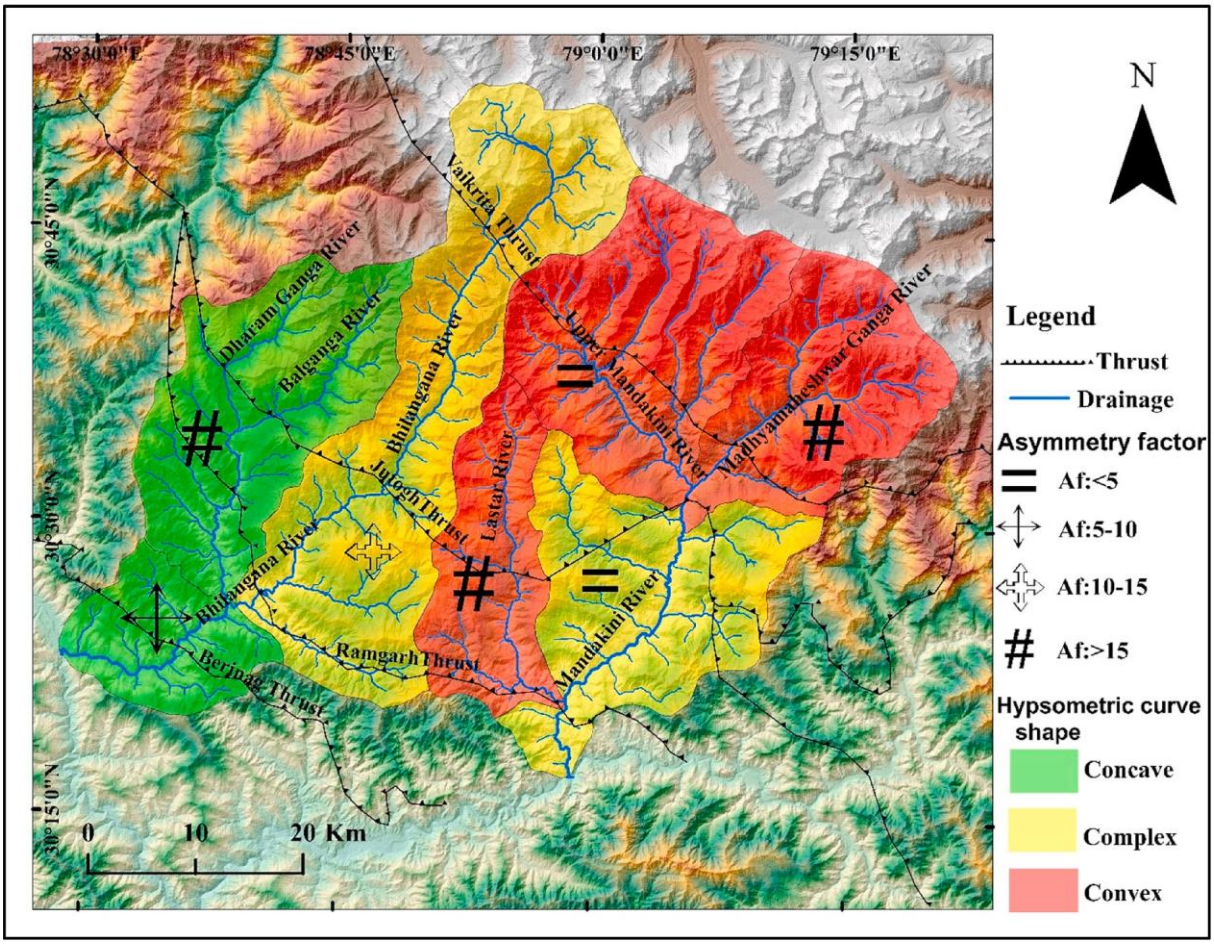

Fig. 4. The basin asymmetry factor and hypsometric curve shapes of the different sub basins.

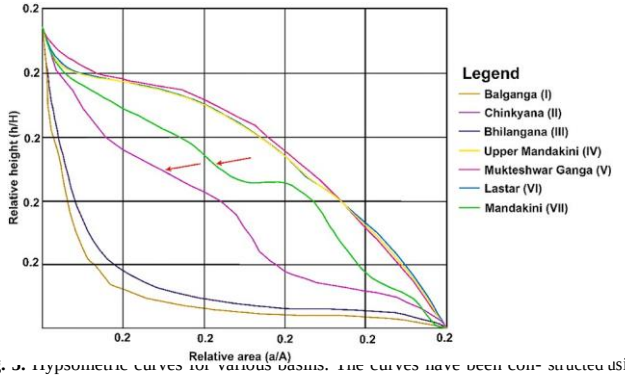

Fig. 5. Hypsometric curves for various basins. The curves have been con- structed using parameters derived from 12.5m resolution DEM. The red arrows depicting the curves illustrating complex hypsometric curves which is seems not be fit either concave or convex curves. (For interpretation of the references to color in this figure legend, the reader is referred to the Web version of this article.)

area below the hypsometric curve is known as the hypsometric integral (HI). The value of HI varies from 0 to 1. These profiles are drawn by projecting rivers onto a theoretical pre-incision surface that is obtained by interpolating the altitudes from present-day lateral divides of the basins.

6.1.4. Steepness index (Ks)

In order to ascertain the fluvial response to terrain instability/sta- bility, the longitudinal river profile provides first-order information to- ward the role of endogenic (tectonics) and exogenic processes (climate) (Hack, 1973; Merrits and Vincent, 1989). Hence in steady state condi- tion, erosion is balanced by uplift; and the longitudinal profile of a river. If there is no differential uplift, the value of Ks should remain constant. However, if the river basin is undergoing differential uplift, Ks may change from one segment to another (Goldrick and Bishop, 2007; Whipple et al., 2013; Joshi et al., 2020). Considering that the channel slope is inversely proportional to drainage basin area, therefore as the drainage area increases, the slope of the river profile decreases.

4. Results and discussion

4.1. Slope and aspect

The slope angle is directly proportional to land instability, as mass movement increases with increase in the slope angle (Taloor et al., 2017). The Himalayan region is highly unstable as this orogenic belt still encounters tectonic rejuvenation which changes the natural relief leading to the modifications in slope angle. Slope is a critical parameter which influences runoff and therefore also on infiltration. The slope map (Fig. 3a) obtained by using the ALOS PALSAR DEM is grouped into seven categories i.e. nearly level (0–1%), very gentle (1–3%), gentle (3–5%), moderate (5–10%), steep (10–15%), moderately steep (15–35%) and very steep (>35%) (Jasrotia et al., 2019; Taloor et al., 2020). The first two categories in the classification are suitable for vegetation and civi- lization growth. Most of the study area is under the level to gentle

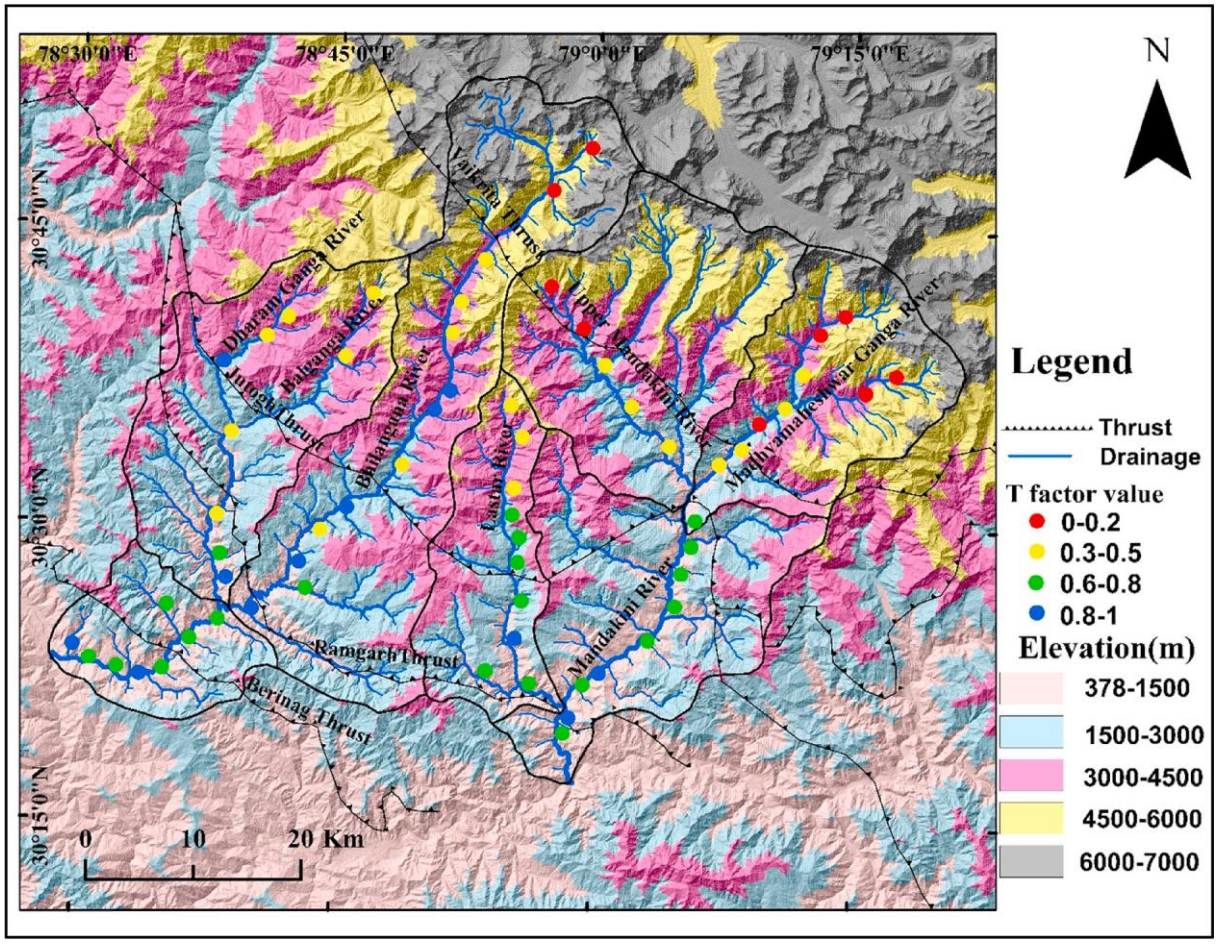

Fig. 6. Topographic symmetry factor map.

category whereas a small portion is under the moderate to steep slope. Besides this a very gentle slope has been observed in the glaciated region located in the northern part of the study area. The central portion of the study area considered to be the area of the lofty mountains where the gradient is high having generally moderate slope and devoid of any major agriculture activity. The major landslides and rock falls on the higher slopes generally occur during the monsoon months. Erosion and mass movement on the uplifted slopes, resulting from reactivation of thrusts and faults, make the region more vulnerable. The monsoon season is where the major landslides and rocks falls in high relief areas occur in the Himalayan region. Further, the reactivation of the thrusts and faults in the region results in the mass movement and erosion.

Aspect is the slope direction which identifies the down slope trend of the maximum rate of change (Fig. 3b). The slope aspect can impact the local climate to a great extent. The aspect map prepared using DEM

indicates the slope direction in counter clock wise from East to South in 90^0 to 360^0.

Most of the study area comes under the north, northeast, west and southwest aspect which indicate the high sunlight on the portion earth surface and relatively more prone to weathering and landslide in the hilly region where the slope is moderate to high and rocks are feasible in nature.

4.2. Morphotectonic analysis

4.2.1. Asymmetric factors (Af)

The basin asymmetry factor is comprehensively used to identify tectonic tilting transverse to flow at basin level. From the obtained re- sults, the Af values are categorized into four classes depending up on their degree of symmetry of the drainage basins. The class-1 indicates AF<5 (nearly symmetrical); class-2 shows AF in the range of 5–10 (minor asymmetry); class-3 falls in the range Af 10–15 (moderately asymmetrical); class-4 is defined if Af >15 (highly asymmetric) (Table 2).

Highly asymmetric values (class-4) were observed in the Lastar, Mukteshwar Ganga, and Chinkyana drainage basins which show sub- stantial shift in the trunk stream because of the tectonic activity (Fig. 4). The Lastar basin show westward tilting, while Mukteshwar Ganga and Chinkyana shows eastward whereas, the upper Mandakini show north- westward asymmetry and the Bhilangana and Mandakini are nearly symmetrical in nature.

4.2.2. Hypsometric curve (HC) and hypsometric integral (HI)

The hypsometric curve estimated for the Upper Mandakini, Lastar and, Muketshwar basins show convex nature which indicates that these basins are relatively young and have undergone minimal erosion. The Balganga and Bhilangana basins display concave nature indicating they have reached the stage of maturity, whereas the Chinkyana and Man- dakini river basins show quite complex curvature indicating tectonic activity (Figs. 4 and 5). High HI value of 0.76 is observed in the Upper Mandakini basin, whereas the lowest value is observed in the Balganga river basin i.e. 0.39.

4.2.3. Transverse topographic symmetry factor (T)

From our analysis it is observed that the higher reaches of the river basins show lower T values and vice versa (Fig. 6). The value of T shows increasing trend while approaching the thrusts existing in the region (Fig. 6). The calculated T values ranges from 0.29 to 0.82 (Table 2).

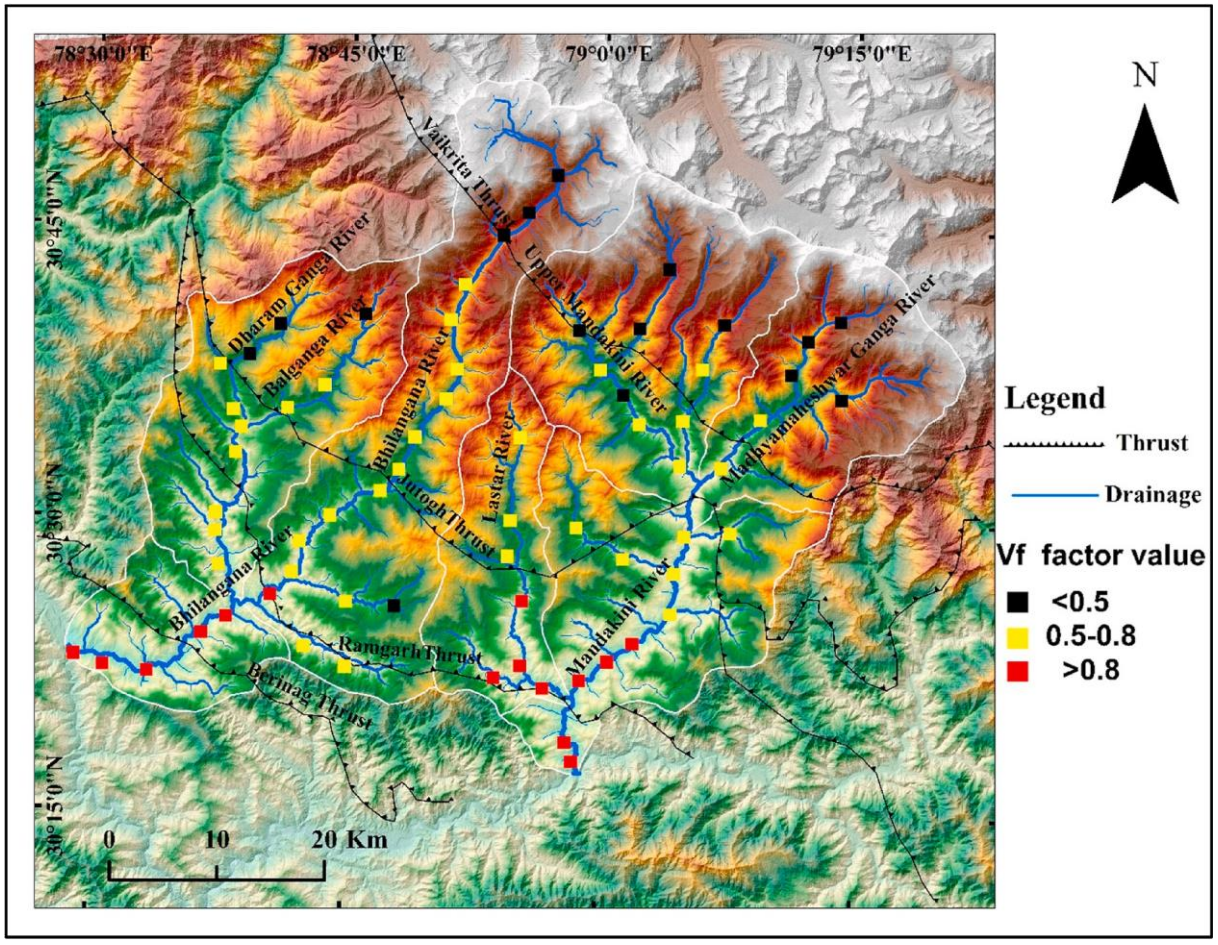

Fig. 7. Valley floor to valley height ratio (Vf) in the sub basin.

4.2.4. Valley floor width to valley height (Vf)

Low values of Vf are observed at the upper reaches of the Balganga, Bhilangana, Upper Mandakini and Madhyamaheswar Ganga rivers where they are intersected by the Vaikrita and Jutogh thrust (Fig. 7). This indicates that these rivers are actively incising. High values of Vf are observed at the intersection of the Ramgarh and Berinag thrust with Bhilangana, Lastar and Mandakini rivers (Fig. 7). This reveals that the upper reaches of these rivers are actively incising and the tectonic ac- tivity gradually decreases approaching the lower reaches.

4.2.5. Stream length gradient index (SL)

The computed SL index values increases abruptly near Vaikrita, Jutogh and Ramgarh Thrust (Fig. 8). The major tributary streams of these sub-basins flow over generally uniform lithology and formations throughout the mid-reaches to upstream segments (Fig. 8). This infor- mation, together with the absence of major Quaternary base-level fluctuations where thrusts are acting as barrier indicates that the high SL activity is caused due to tectonic activity.

4.2.6. Assessment of longitudinal river profile and knickpoints

The longitudinal river profiles of the Mandakini and Bhilangana was constructed using the elevation and downstream distance (Figs. 9a–10a). The gradient change along the course of a river has been assumed to be formed by tectonic uplift along the major thrusts/faults. The Mandakini and Bhilangana River shows concave-convex-concave shaped profile suggesting disequilibrium state of river channel (Figs. 9a–10a). To delineate the knickpoints along the Mandakini and Bhilangana river basins, longitudinal profiles (elevation vs distance) were compared with drainage area and slope-area (log-log) plots (Figs. 9b–10b). The breaks in slope area plot were correlated with sudden variations of drainage area with distance, and marked as knickpoints in the river profile (Figs. 10a–11a).

Furthermore, slope-area plots for the basin were analyzed in three river basins (Figs. 9b–10b) to estimate normalized (ksn). The $\theta ref = -0.45$ was used for calculation of ksn. The ksn values at θref vary be- tween 50 and 500 for Bhilangana (Fig. 9c–d), where ksn values at θref for Mandakini ranges between 100 and 550 (Fig. 10c–d). There is a significant difference in concavity values which affect the steepness of the basin. This change of ksn values estimated at θref can be used to compare the changes in basin slope. The lowest values of ksn at θref observed for Mandakini and Bhilangana River basins are interpreted as a lithological contrast and tectonic control on the drainage system. It has been observed that distinction between the transient behavior of rivers caused by tectonics or climate is not obvious in the slope-area plot (Whittaker, 2007). Wobus et al. (2006) suggested that the tectonic ele- ments over the steepness can be explained by a plan view of the basin (see also Kirby et al., 2003). The knickpoints are analyzed in the plan view of the Mandakini and Bhilangana, which is accomplished by overlapping the ksn plot obtained for all major tributaries of the River basins and the lithology as well as structures. These two spatial values are then imposed over DEM for each basin and a well-defined knick point clustering was found in the vicinity of major thrusts (Fig. 9a–dand 10a-d-f). Along the Bhilangana River, a total of 45 knick points were identified in the vicinity of the major thrusts/faults. Whereas along the Mandakini River a total 105 knickpoints were identified.

4.2.7. Examination of river gradient, steepness and Chi

The χ plot of Mandakini and Bhilangana river basin was constructed

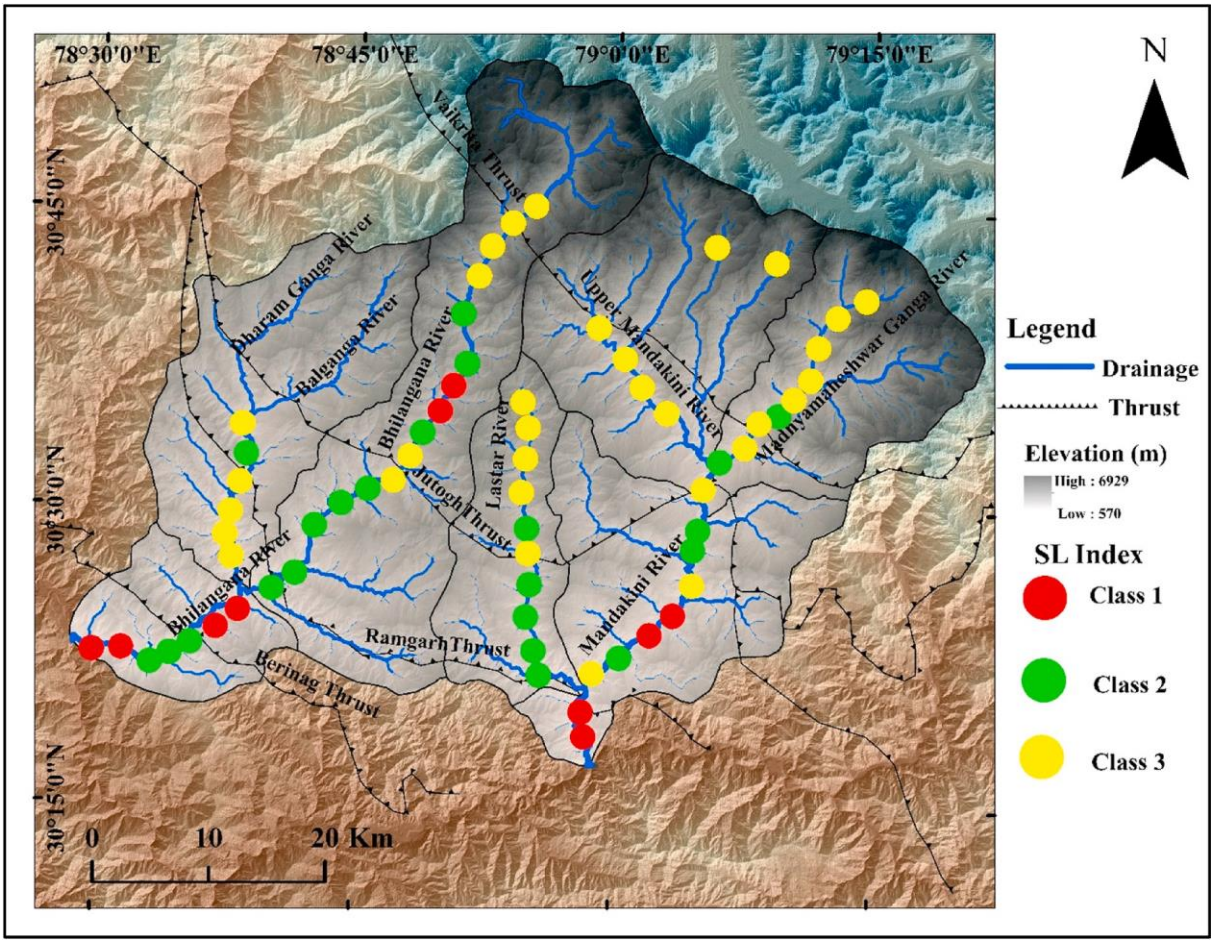

Fig. 8. Stream length gradient index computed over different sub basins.

after extracting the flow grid, flow accumulation, flow direction and upstream drainage area from the DEM data using MATLAB software. To identify flow direction and paths, the pits and depressions were filled to find the steepest flow direction and removal of local anomalies from the DEM. To determine the χ for entire Mandakini and Bhilangana drainage basins, values of m/n were selected. To reduce the scattering of pixel, the best fit concavity and m/n was decided after construction of several χ plots, which provided a range of m/n values for the whole basin. The best fit value of m/n ratio is chosen where the main stream collapses with tributary streams within the basin as also proposed by (Perron and Royden, 2013). The χ plot shows best fit m/n ratio ranging from 0.40 to 0.45, therefore the most satisfying value of m/n ratio 0.44 was selected for the basin. The χ plots of the main stream and tributary streams of Mandakini and Bhilangana River, diverging from linearity and have convexity (zone of uplift) and concavity (zone of erosion) in their lon- gitudinal profile (Fig. 10c–f). Such a diverging nature of profile indicates that the river basins are not in the steady state of equilibrium and behave according to the lithology and tectonics. In steady state condition, the channels are forced to move toward the equilibrium condition (Kothyari et al., 2020a). The influence of climate, lithology and tectonics in the drainage pattern has been illustrated by equilibrium profile of a river (Kothyari et al., 2020a). The changes in χ plot are highlighted by the state of disequilibrium, where fractional increase or decrease of up- stream area can be observed with respect to steady-state trend line (Joshi et al., 2020; Kothyari et al., 2020a and references there in). The drainage area and length of profile increase with increasing and decreasing χ values and simultaneously migrate above and below the steady-state line of χ plot (Fig. 10c). The drainage pattern migration located above the steady-state line on a χ plot experiences more erosion than the tectonic uplift (Royden, and Perron, 2013), whereas, a channel below the steady-state trend experiences less erosion and faster tectonic uplift. The χ plot of Mandakini and Bhilangana basin clearly shows in- crease of drainage area with faster erosion and length above and decreasing with lower erosion of the length below the steady state trend line (Fig. 10c–f).

4.3. Rainfall and temperature

The rainfall and temperature data acquired from the Indian Water Portal (IWP) from 1900-2001 reveals that the precipitation has been gradually decreasing in the Garhwal region, whereas the temperature is increasing over the past hundred years (Fig. 11 and Fig. 12a,- b). The results are persuasive of a credible that increase in the temperature and precipitation have resulted in the change of landscape and morphology of the sub basins due to flooding which extremely affected the flora fauna and Holocene civilization.

4.4. Geomorphological evidences of landforms development along the Bhilangana valley

Since rock uplift is ultimately the engine driving relief production in active orogens (Wobus et al., 2006). Any change in the relief due to tectonic and climate can form the different landforms. The previous studies on the neotectonic, hill slopes, rivers dynamics suggest the several types of landforms developed all along the active thrusts and faults (Nakata, 1989; Valdiya, 1993; Valdiya et al., 1996; Bookhagen et al., 2005; Goswami and Pant, 2008; Luirei et al., 2012, 2015; Pathak et al., 2013; Dumka et al., 2014; Joshi and Kotlia, 2015; Joshi et al.,

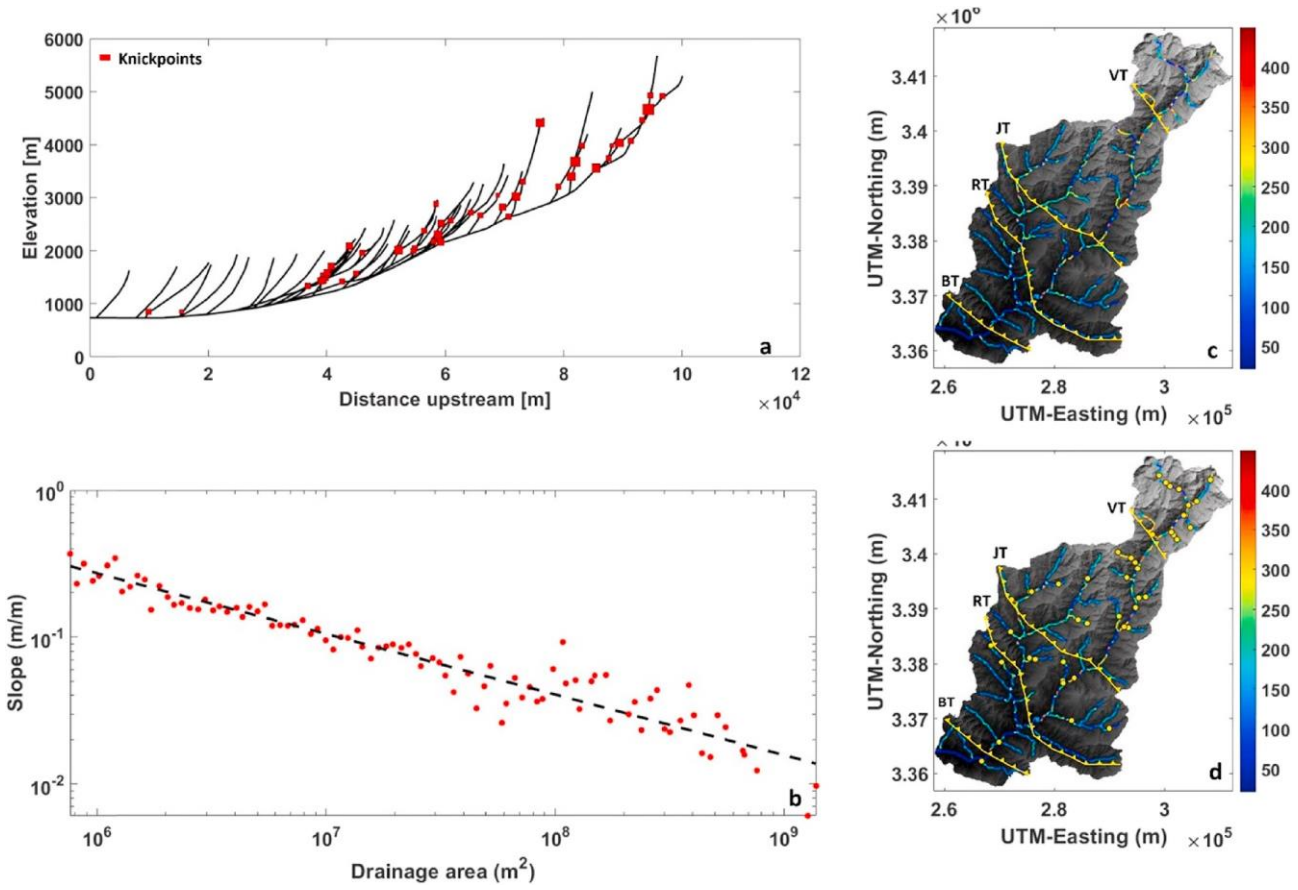

Fig. 9. (a). Longitudinal profile (elevation vs distance) of Bhilangana river basin. The knickpoint plotted along the long profile are marked by red color. (b) Slope vs drainage area for plot for Bhilangana River at (θ_{ref}) at 0.45 (c) Ksn map of Bhilangana basin at normalized concavity (θ) at 0.45 showing steepness changes within the basin. (d) The combined Ksn and knickpoints map of Bhilangana basin.

2016; Kotlia et al., 2017; Asthana et al., 2018; Bisht et al., 2020). These features are active and stabilized landslides, uplifted paired or unpaired terraces, modification of valley channels, incision, development of gorges and waterfalls, entrenched meandering and offsetting of the older faults by the later formed ones, etc. The regional geomorphology of the area is also characterized by high relief and moderately dissected topography carved into high ridge and deep valley setting (Chaudhary et al., 2010). In present investigation numbers of geomorphic features are observed such as fluvial terraces, entrenched stream course, landslide-induced ponding, and active and stabilized landslide deposits which suggest geomorphic development along the Bhilangana and Mandakini Rivers mainly around Chamiyala region, along Balganga
Valley (Fig. 13a–f). We attribute their development to the activity along the Ramgarh thrust, Almora thrust and Vaikrita thrust which mark the
south and the north boundary of the study area. The active landslide fans also suggesting the active nature of existing thrusts and lineament of the area. At least three to four fluvial terraces are recognized along the right bank tributary of Balganga River near Aragarh with the total elevation difference of 70m covered by the erosion terrace. Further, downstream at 2 to 3 levels of river terraces are documented along both the banks of the stream Sunar Gaon. There are five levels of river terraces in the right bank of Balganaga River are envisaged near Maikot-Raj Gaon area with an elevation different of 138m. The elevation of T1 terrace is 964 m, while the T5 terrace is about 1024. Further downwards an entranced meandering was observed and the river becomes very wide and flow in the almost straight river course along with three-four levels (T_1-T_4, T_4 being the oldest) of river terraces registering elevation difference of 42 m between Chamiyala and Baleshwer where the most human settlement is observed. Other than the river terraces, the fault facet, river ponding,

active and stabilized landslides was documented in and around Cha- miyala area. The terrace deposits with toe cutting are well recognized between Lata-Chamiyala-Baleshwer sectors. Further, it is also suggested that the Bhilangana River flow along the faulted course which has dis- placed the MCT around Ghansyali area (Singh and Sakalani, 1978). The several fresh landslides observed in this zone (Fig. 14 and b) also show the activeness of the area as fresh landslide debris and river toe cutting also point to the active nature of faults (Bhakuni et al., 2013) as it is mentioned the geomorphic equilibrium in the neotectonic fault region (Wobus et al., 2006).

4.5. Regional seismicity and geodetic study

The Kumaun and Garhwal central Himalaya has undergone extensive tectonic deformation in the geological past. The area is seismically active as followed by intra crustal boundary thrusts as well as subsidiary faults (Gansser, 1964; Tapponnier and Molnar, 1977; Valdiya, 1980; Dumka et al., 2014). The Garhwal Himalaya is located within a seismic gap (Khattri and Tyagi, 1983; Khattri, 1987), small and moderate magnitude earthquakes and severe landslides have frequently occurred here in recent times (Sarkar et al., 2001). Majority of earthquakes in the central Himalaya is the shallow focus (Kumar et al., 2012). Frequently occurring moderate earthquakes, magnitude between 5 and 7 is distributed close to the MCT zone and northern part of the Lesser Himalaya (Thakur, 2004: Khatri et al., 1989). The ongoing tectonic movements are also responsible for the modifications in the topography
i.e. making the terrain extremely rugged and difficult (Valdiya, 1999). Ongoing crustal deformation and adjustments are well reflected by two major earthquakes in the vicinity of Bhilangana and Mandakini basin,

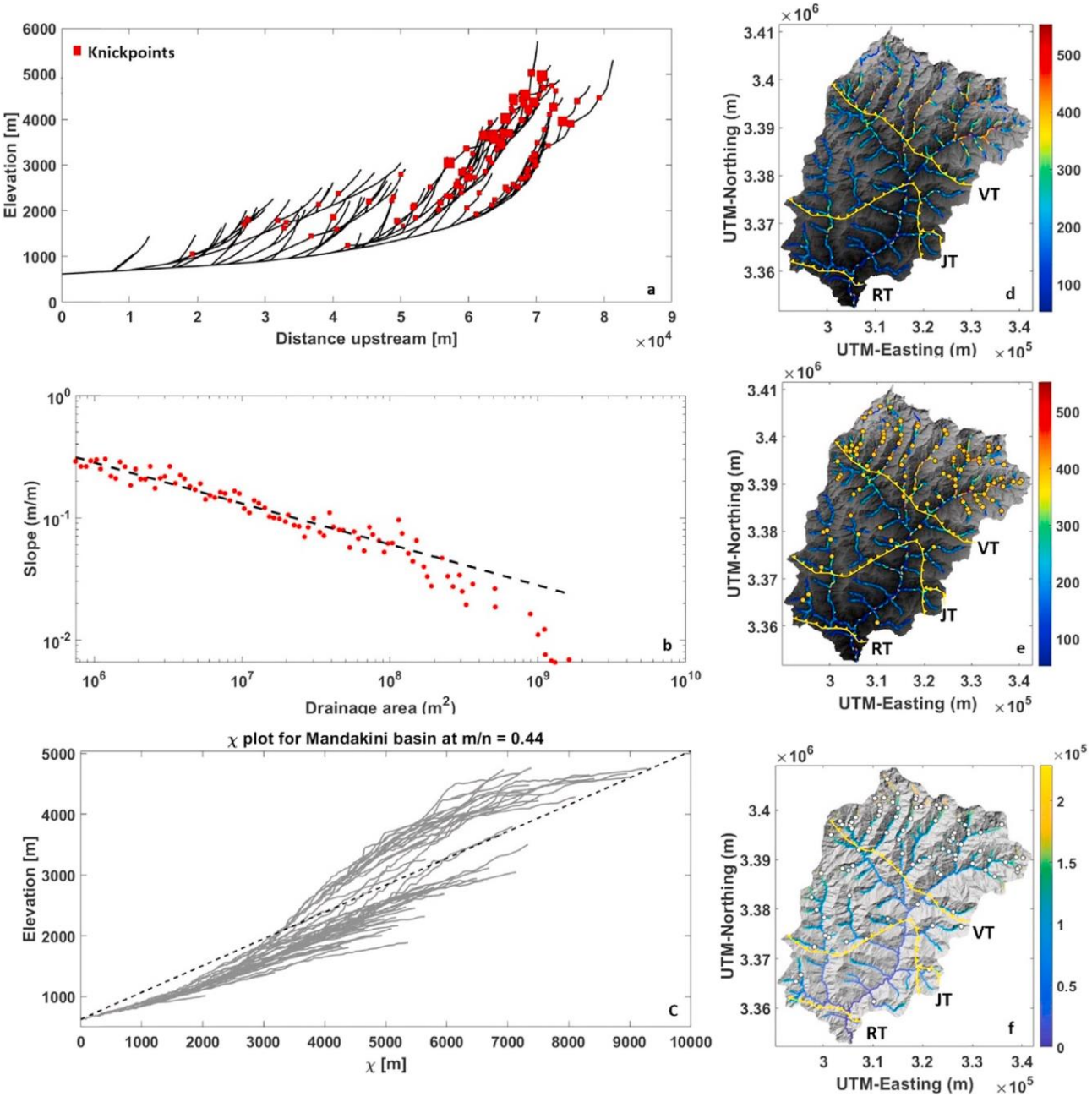

Fig. 10. (a). Longitudinal profile (elevation vs distance) of Mandakini river basin. The knickpoint plotted along the long profile are marked by red color. 11(b) Slope vs drainage area for plot for Mandakini River at (θref) at 0.45, (c) Analytical calculation showing effect of drainage area changes on Chi (χ) at concavity m/n 0.44 (d) Ksn map of Mandakani basin at normalized concavity (θ) at 0.45 showing steepness changes within the basin. (e) The combined Ksn and knickpoints map of Mandakini basin, (f) Map showing χ values of Mandakini basin at concavity m/n 0.44, the knickpoints on χ plot are marked by red color. (For interpretation of the references to color in this figure legend, the reader is referred to the Web version of this article.)

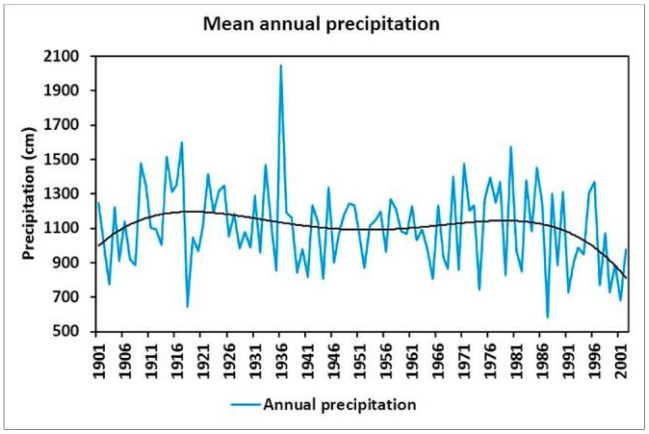

Fig. 11. Annual mean precipitation.

such as, 1991 Uttarkashi (Mw 6.8) and 1999 Chamoli (Mw 6.6). The Garhwal-Kumaun region continues to accumulate the built-up of strain energy (Paul, 2010) and makes the region more prone to large earth- quake in future (Bilham and Ambrseys, 2005). Further, the GPS (Global Positioning System) Geodesy is used to study the convergence rate and tectonic deformation (Dumka et al., 2020). Recent geodetic measure- ments in the in the Tons valley, Garhwal Himalaya have shown signif- icant ground deformation in the thrust zone (Valdiya, 1981). Convergence rates in Garhwal-Kumaun Himalayas are 10–18 mm/yr (Jade et al., 2004). The seismic map of the Kumaun-Garhwal region based on USGS, ISC, IMD data source suggesting the Pithoragarh-Bageshwer-Joshimath-Uttarkashi regions along the zone of Vaikrita/MCT is most active. The cluster of seismic events ($M < 5$) recorded along the MCT indicates the present-day deformation (Jade et al., 2017). The maximum of extensional and compressional strains due to the force acting along the MCT in the NW–SE direction is found to be 0.4 and 0.1ч strain/yr, respectively (Ponraj et al., 2010). Epicentral distribution map of Kumaun-Garhwal region also shows cluster around Ghansali-Chamiyala region (Fig. 15). The documented seismic event along with the development of various geomorphic features is clear indication of the active nature of thrusts/faults within the area.

5. Conclusion

Tectono-geomorphic investigation of the Mandakini and Bhilangana drainage basins of Garhwal region elucidate that these basins have been subjected to an increase of tectonic activity since 5 Ma resulting in the rapid uplift of terrain which probably continues up to the present. The topography is still evolving while adjusting to disequilibrium caused by changes in tectonic boundary conditions, and active folding within the Mandakini and Bhilangana thrust belts would still be persistent. The slope is moderate to high in most of the study area which also speed up the landslide and avalanches in the study area which is further sup- ported by the feasible nature of the rocks in the study area. Bearing in mind the rapid erosion rates affecting these basins expressions of tec- tonics could be maintained only if the topography is considerably young and are diagnostic of regions undergoing rapid tectonic uplift. The re- sults of the geomorphic indices show that the active Mukteshwar Ganga highest asymmetric basin while the Mandakini is a least asymmetric basin. Based on the hypsometric curve it is inferred that the upper Mandakini basin is relatively young and weakly eroded, tectonically very active in nature which has been subjected to large numbers of landslides, debris flow highly affected portion of the 2013 Kedarnath tragedy. The drainage morphology of Bhilangana and Mandakini of the central Himalaya is considerably modified by tectonic and subordinate climatic processes as evident from variations in k_{sn} and χ anomalies. The k_{sn} and χ values reveals that the gradient changes along the longitudinal length of drainage basin is attributed to the formation of knickpoints.

The Muktheswar Ganga river have the lowest Vf ratio which indicates that the western portion of the study area is prone to be tectonically active in nature and the seismic data of the Garhwal Himalayas also put forward the idea that the Upper Eastern Ganga river (Muktheswar Ganga) was prone to more seismic hazard in the past. The active and stabilized landslides, uplifted unpaired terraces, modification of valley channels, incision of rivers, development of gorges and waterfalls, entrenched meandering and offsetting of the older faults indicates that are under investigation is tectonically active.

Additional information

All the authors have made contribution to this manuscript. There is no conflict of interest among all co-authors.

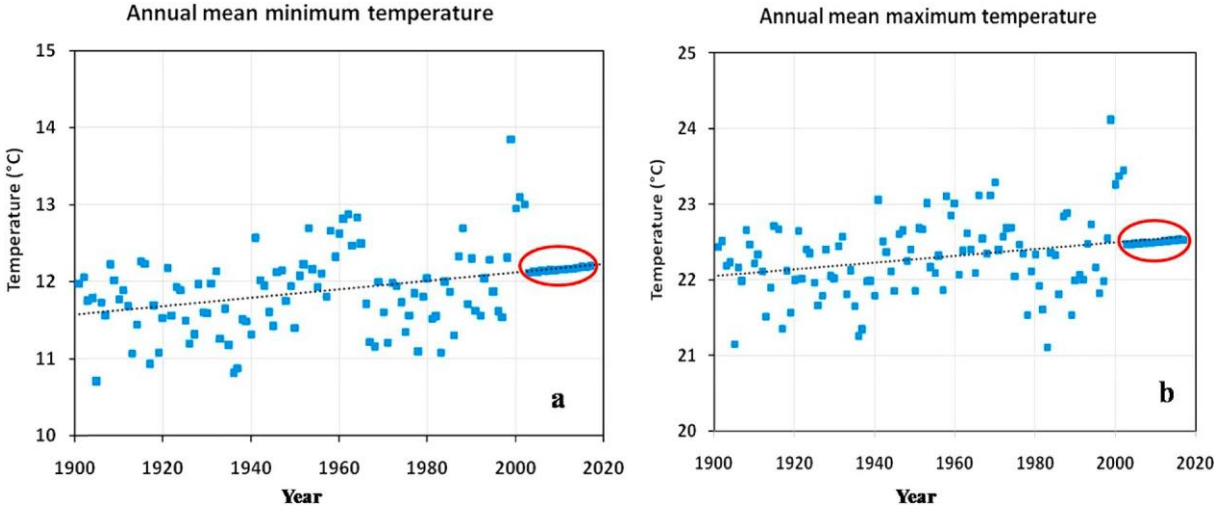

Fig. 12. Average annual minimum temperature (a), maximum temperature (b) from 1901 to 2017 (data derived from India Water Portal (IWP) having data record from 1901 to 2002). For 2003 to 2017, the values were obtained using the existing trend in the longterm data. The data points with dotted ellipses show extrap- olated values.

Fig. 13. (a) Four levels of fluvial terraces Near Aragarh, Sunargaon along a tributary of Balganga Near Chamiyala (b) Five levels of river terraces in the right bank of Balganga River near Maikot-Raj Gaon area (c) Entrenched meandering and river terraces along left bank of Balganaga downstream of Maikot-Raj Gaon area; (d) Google image shows the wide and straight course of river along with development of fluvial terraces between Chamiyala-Baleshwar area; (e) Fault facet Near Sunargaon: (f) River ponding downstream of Baleshwar.

Fig. 14. (a) Tilted Tree and retaining walls show recent activity along stabilized landslide material (b) River toe cutting near Lata village along Balganga valley.

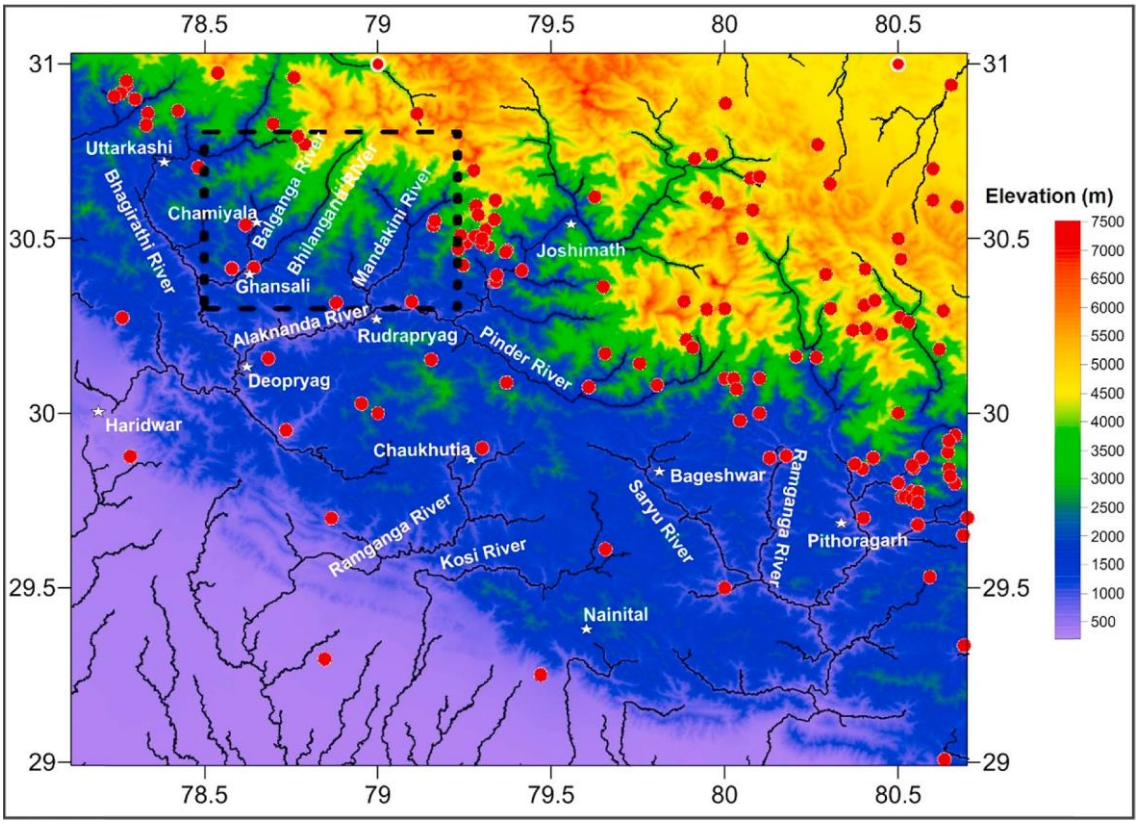

Fig. 15. Epicentral distribution map of Kumaun and Garhwal region superimposed over the DEM.

Declaration of competing interest

The authors declare that they have no known competing financial interests or personal relationships
That could have appeared to influence the work reported in this paper.

Acknowledgement

The AKT is highly thankful to the Head, Department of Remote Sensing& GIS,andUniversityofJammuforconsistentsupporttocarry out this research work. We are thankful to reviewers for their constructive comments in improving the manuscript.

References

Alam, A., Bhat, M.S., Kotlia, B.S., Ahmad, B., Ahmad, S., Taloor, A.K., Ahmad, H.F., 2017. Coexistent pre-existing extensional and subsequent compressional tectonic deformation in the Kashmir basin, NW Himalaya. Quat. Int. 444, 201–208.

Alam, A., Bhat, M.S., Kotlia, B.S., Ahmad, B., Ahmad, S., Taloor, A.K., Ahmad, H.F., 2018. Hybrid tectonic character of the Kashmir basin: response to comment on "Coexistent pre-existing extensional and subsequent compressional tectonic deformation in the Kashmir basin, NW Himalaya (Alam et al., 2017)" by Shah (2017). Quat. Int. 468, 284–289.

Asthana, A.K.L., Luirei, K., Kothyari, G.C., Pandey, P., 2018. Quantitative analysis of nayar river basin, garhwal outer lesser Himalaya: implication to neotectonic activity. Himal. Geol. 39 (1), 57–67.

Bahuguna, V.K., Saklani, P.S., 1988. Tectonics of the main central thrust in Garhwal Himalaya. J. Geol. Soc. India 31, 197–209.

Bhakuni, S.S., Luirei, K., Kothyari, G.C., 2013. Neotectonic Fault in the middle part of Lesser Himalaya, Arunachal Pradesh: a study based on structural and morphotectonic analyses. Himal. Geol. 34 (1), 57–64.

Bhat, M.S., Alam, A., Ahmad, B., Kotlia, B.S., Farooq, H., Taloor, A.K., Ahmad, S., 2019. Flood frequency analysis of river Jhelum in Kashmir basin. Quat. Int. 507, 288–294. https://doi.org/10.1016/j.quaint.2018.09.039.

Bilham, R., Ambraseys, N., 2005. Apparent Himalayan slip deficit from the summation of seismic moments for Himalayan earthquakes, 1500-2000. Current Sci. India 88 (10), 1658–1663.

Bisht, H., Kotlia, B.S., Kumar, K., Dumka, R.K., Taloor, A.K., Upadhyay, R., 2020. GPS derived crustal velocity, tectonic deformation and strain in the Indian Himalayan arc. Quat. Int. https://doi.org/10.1016/j.quaint.2020.04.028.

Bookhagen, B., Thiede, R.C., Strecker, M.R., 2005. Late Quaternary intensified monsoon phases control landscape evolution in the northwest Himalaya. Geology 33, 149–152.

Brookfield, M.E., 1993. The himalayan passive margin from precambrian to cretaceous. Sediment. Geol. 84, 1–35.

Bull, W.L., Knuepfer, P.L., 1987. Adjustments by the Charwell River, New Zealand, to uplift and climatic changes. Geomorphology 1 (1), 151–32.

Bull, W.B., McFadden, L.D., 1977. Geomorphology in Arid Regions. Geomorphology in Arid Regions.

Burbank, D.W., Anderson, R.S., 2001. Tectonic Geomorphology. Blackwell Science, p. 274.

Chaudhary, S., Gupta, V., Sundriyal, Y., 2010. Surface and sub-surface characterization of byung landslide in Mandakini valley, garhwal Himalaya. Himal. Geol. 31 (2), 1251–132.

Choubey, V.M., Ramola, R.C., 1997. Correlation between geology and radon levels in groundwater, soil and indoor air in Bhilangna Valley, Garhwal Himalaya, India. Environ. Geol. 32 (4), 2581–262.

Dubey, R.K., Dhar, J.A., Kothyari, G.C., 2017. Evaluation of relative tectonic perturbations of the Kashmir Basin, Northwest Himalaya, India: an integrated morphological approach. J. Asian Earth Sci. 148, 153–172.

Dumka, R.K., Kotlia, B.S., Kumar, K., Satyal, G., Joshi, L.M., 2014. Crustal deformation revealed by GPS in Kumaun Himalaya, India. J. Mt. Sci. 11 (1), 41–50.

Dumka, R.K., SuriBabu, D., Taloor, A.K., Prajapati, S., Kotlia, B.S., 2020. Demarcation of solar cycle 24 and characterization of Ionospheric GPS-TEC towards the Western part of India. Quat. Int. https://doi.org/10.1016/j.quaint.2020.04.051.

Dumont, J.F., Santana, E., Vilema, W., 2005. Morphologic evidence of active motion of the zambapala fault, gulf of guayaquil (Ecuador). Geomorphology 65, 223–239.

Gansser, A., 1964. The Geology of the Himalayas. Wiley Interscience, New York, p. 289. Giaconia, F., Booth-Rea, G., Martínez-Martínez, J.M., Azañ̃n, J.M., P̃rez-Pena, J.V., P̃rez-Romero, J., Villegas, I., 2012. Geomorphic evidence of active tectonics in the Sierra Alhamilla (eastern Betics, SE Spain). Geomorphology 145, 90–106.

Godin, L., 2003. Structural evolution of the Tethyan sedimentary sequence in the Annapurna area, central Nepal Himalaya. J. Asian Earth Sci. 22, 307–328.

Goldrick, G., Bishop, P., 2007. Regional analysis of bedrock stream long profiles: evaluation of Hack's SL form, and formulation and assessment of an alternative (the DS form). Earth Surf. Process. Landforms 32 (5), 649–671.

Goswami, P.K., Pant, C.C., 2008. Morphotectonic evolution of the binau-ramganga-naurar transverse valley, southern Kumaun lesser Himalaya. Curr. Sci. 94, 1640–1645.

Gupta, S., 1997. Himalayan drainage patterns and the origin of fluvial mega fans in the Ganges foreland basin. Geology 25, 11–14.

Hack, J.T., 1973. Stream-profiles analysis and stream-gradient index. J. Res. U. S. Geol. Surv. 1, 421–429.

Hajam, R.A., Hamid, A., Bhat, S., 2013. Application of morphometric analysis for geo-hydrological studies using geo-spatial technology-A case study of Vishav Drainage Basin. Hydrol. Curr. Res. 4–157, 1–12.

Haque, S., Kannaujiya, S., Taloor, A.K., Keshri, D., Bhunia, R.K., Ray, P.K.C., Chauhan, P., 2020. Identification of Groundwater Resource Zone in the Active Tectonic Region of Himalaya through Earth Observatory Techniques. Groundwater for Sustainable Development, 100337. https://doi.org/10.1016/j.gsd.2020.100337.

Hilley, G.E., Arrowsmith, J.R., 2008. Geomorphic response to uplift along the Dragon's Back pressure ridge, Carrizo Plain, California. Geology 36 (5), 367–370.

Hodges, K.V., Wobus, C., Ruhl, K., Schildgen, T., Whipple, K., 2004. Quaternary deformation, river steepening, and heavy precipitation at the front of the Higher Himalayan ranges. Earth Planet Sci. Lett. 220 (3–4), 379–389.

Holbrook, J., Schumm, S.A., 1999. Geomorphic and sedimentary response of rivers to tectonic deformation: a brief review and critique of a tool for recognizing subtle epeirogenic deformation in modern and ancient settings. Tectonophysics 305 (1–3), 287–306.

Horton, R.E., 1945. Drainage Basin Characteristics, Transactions, vol. 13. American Geophysical Union, pp. 350–361.

Jackson, J., Leeder, M., 1994. Drainage systems and the development of normal faults: an example from Pleasant Valley, Nevada. J. Struct. Geol. 16 (8), 1041–1059.

Jade, S., Bhatt, B.C., Yang, Z., Bendick, R., Gaur, V.K., Molnar, P., Anand, M.B., Kumar, D., 2004. GPS measurements from the Ladakh Himalaya, India: preliminary tests of plate-like or continuous deformation in Tibet. Geol. Soc. Am. Bull. 116 (11–12), 1385–1391.

Jade, S., Shrungeshwara, T.S., Kumar, K., Choudhury, P., Dumka, R.K., Bhu, H., 2017. India plate angular velocity and contemporary deformation rates from continuous GPS measurements from 1996 to 2015. Sci. Rep. 7, 11439. https://doi.org/10.1038/ s41598-017-11697-w.

Jasrotia, A.S., Kumar, A., Taloor, A.K., Saraf, A.K., 2019. Artificial recharge to groundwater using geospatial and groundwater modelling techniques in North Western Himalaya, India. Arabian J. Geosci 12, 774. https://doi.org/10.1007/ s12517-019-4855-5.

Joshi, L.M., Kotlia, B.S., 2015. Neotectonically triggered instability around the palaeolake regime in Central Kumaun Himalaya, India. Quat. Int. 371, 219–223.

Joshi, L.M., Pant, P.D., Kotlia, B.S., Kothyari, G.C., Luirei, K., Singh, A.K., 2016. Structural overview and morphotectonic evolution of a strike slip fault in the zone of North Almora Thrust, Central Kumaun Himalaya, India. J. Geol. Research. https:// doi.org/10.1155/2016/6980943.

Joshi, N., Kothyari, G.C., Pant, C.C., 2020. Drainage conformation and transient response of river system in thrust segmentation of Northwest Himachal Himalaya, India. Quat. Int. https://doi.org/10.1016/j.quaint.2020.05.024.

Juyal, N., Sundriyal, Y., Rana, N., Chaudhary, S., Singhvi, A.K., 2010. Late Quaternary fluvial aggradation and incision in the monsoon-dominated Alaknanda valley, Central Himalaya, Uttrakhand, India. J. Quat. Sci. 25 (8), 1293–1304.

Kannaujiya, S., Gautam, P.K.R., Chauhan, P., Roy, P.N.S., Pal, S.K., Taloor, A.K., 2020. Contribution of seasonal hydrological loading in the variation of seismicity and geodetic deformation in Garhwal region of Northwest Himalaya. Quat. Int. https:// doi.org/10.1016/j.quaint.2020.04.049.

Keller, E.A., Pinter, N., 1996. Active Tectonics: Earthquakes, Uplift, and Landscape. Prentice Hall, New Jersey.

Keller, E.A., Pinter, N., 2002. Active Tectonics: Earthquakes, Uplift, and Landscape, second ed. Prentice Hall, New Jersey, pp. 1–362.

Khan, A., Govil, H., Taloor, A.K., Kumar, G., 2020. Identification of Artificial Groundwater Recharge Sites in Parts of Yamuna River Basin India Based on Remote Sensing and Geographical Information System. Groundwater for Sustainable Development, p. 100415.

Khattri, K.N., 1987. Great earthquakes, seismicity gaps and potential for earthquake disaster along the Himalaya plate boundary. Tectonophysics 138 (1), 79–92.

Khattri, K.N., Tyagi, A.K., 1983. Seismicity patterns in the Himalayan plate boundary and identification of the areas of high seismic potential. Tectonophysics 96, 281–297.

Khattri, K.N., Chander, R., Gaur, V.K., Sarkar, I., Kumar, S., 1989. New seismological results on the tectonincs of the Garhwal Himalaya. Proc. Indiana Acad. Sci. 98, 91–109.

Kirby, E., Whipple, K., Tang, W., Chen, Z., 2003. Distribution of active rock uplift along the eastern margin of the Tibetan Plateau, Inferences from bedrock channel longitudinal profiles. J. Geophys. Res. 108, B4. https://doi.org/10.1029/ 2001JB000861.

Knight, J., Grab, S.W., 2018. Drainage network morphometry and evolution in the eastern Lesotho highlands, southern Africa. Quat. Int. 470, 4–17.

Kothyari, G.C., 2014. Morphometric analysis of tectonically active pindar and saryu river basins: central Kumaun Himalaya. Zeitschrift für fur Geomorphologie 59 (4), 421–442.

Kothyari, G.C., Luirei, K., 2016. Late quaternary tectonic landforms and fluvial aggradation in the saryu river valley: central Kumaun Himalaya. Geomorphology 268, 159–176.

Kothyari, G.C., Rastogi, B.K., Morthekai, P., Dumka, R.K., 2016a. Active segmentation assessment of the tectonically active south wagad fault in kachchh western peninsular India. Geomorphology 253, 491–507.

Kothyari, G.C., Rastogi, B.K., Morthekai, P., Dumka, R.K., 2016b. Landform development in a zone of active Gedi Fault Eastern Kachchh rift basin India. Tectonophysics 670, 115–126.

Kothyari, G.C., Kandregula, R.S., Luirei, K., 2017a. Morphotectonic records of neotectonic activity in the vicinity of north Almora thrust zone central Kumaun Himalaya. Geomorphology 285, 272–286.

Kothyari, G.C., Shukla, A.D., Juyal, N., 2017b. Reconstruction of late quaternary climate and seismicity using fluvial landforms in pindar river valley, central Himalaya, Uttarakhand, India. Quat. Int. 443, 248–264.

Kothyari, G.C., Singh, A.P., Mishra, S., Kandregula, R.S., Chaudhary, I., Chauhan, G., 2018a. Evolution of drainage in response to brittle - ductile dynamics and surface processes in Kachchh Rift Basin, Western India. In: Evgenii Vitalievich Sharkov 2018). Tectonics. Intech Publication, ISBN 978-953-51-5619-2.

Kothyari, G.C., Kandregula, R.S., Luirei, K., 2018b. Response: discussion of 'Morphotectonic records of neotectonic activity in the vicinity of North Almora Thrust Zone, Central Kumaun Himalaya' by Kothyari et al. (2017). Geomorphology (285), 272–286. Geomorphology 301, 153-166.

Kothyari, G.C., Joshi, N., Taloor, A.K., Kandregula, R.S., Kotlia, B.S., Pant, C.C., Singh, R. K., 2019. Landscape evolution and deduction of surface deformation in the Soan Dun, NW Himalaya, India. Quat. Int. 507, 302–323.

Kothyari, G.C., Kotlia, B.S., Talukdar, R., Pant, C.C., Joshi, L.M., 2020a. Evidences of neotectonic activity along goriganga river, higher central Kumaun Himalaya. India Geol. J. https://doi.org/10.1002/gj.3791.

Kothyari, G.C., Pant, P.D., Talukdar, R., Taloor, A.K., Kandregula, R.S., Rawat, S., 2020b. Lateral variations in sedimentation records along the strike length of north Almora thrust: central Kumaun Himalaya. Quat. Sci. Adv. https://doi.org/10.1016/j. qsa.2020.100009.

Kotlia, B.S., Goswami, P.K., Joshi, L.M., Singh, A.K., Sharma, A.K., 2017. Sedimentary environment and geomorphic development of the uppermost siwalik molasse in Kumaun himalayan foreland basin, north India. Geol. J. https://doi.org/10.1002/ gj.2883.

Kumar, N., Paul, A., Mahajan, A.K., Yadav, D.K., Bora, C., 2012. The Mw 5.0 Kharsali, Garhwal Himalayan earthquake of 23 July 2007: source characterization and tectonic implications. Curr. Sci. 102, 1674–1682.

Kumar, D., Singh, A.K., Taloor, A.K., Singh, D.S., 2020. Recessional pattern of thelu and swetvarn glaciers between 1968 and 2019, Bhagirathi basin, garhwal Himalaya, India. Quat. Int. https://doi.org/10.1016/j.quaint.2020.05.017.

Lave, J., Avouac, J.P., 2001. Fluvial incision and tectonic uplift across the Himalayas of central Nepal. J. Geophys. Res.: Solid Earth 106 (B11), 26561–26591. https://doi. org/10.1029/2001JB000359.

Lefort, P., 1996. Evolution of the Himalaya. In: Yin, A., Harrison, T.M. (Eds.), The Tectonics of Asia. Cambridge University Press, New York, pp. 95–106.

Luirei, K., Bhakuni, S.S., Srivastava, P., Suresh, N., 2012. Late pleistocene – Holocene tectonic activities in the frontal part of NE Himalaya between siang and dibang valleys, Arunachal Pradesh, India. Z. Geomorphol. 56, 477–493.

Luirei, L., Bhakuni, S.S., Kothyari, G.C., Tripathi, K., Pant, P.D., 2015. Quaternary extensional and compressional tectonics revealed from quaternary landforms along kosi river valley, outer Kumaun lesser Himalaya, Uttarakhand. Int. J. Earth Sci. https://doi.org/10.1007/s00531-015-1204-0.

Men�ndez, I., Silva, P.G., Martín-Betancor, M., P�rez-Torrado, F.J., Guillou, H., Scaillet, S., 2008. Fluvial dissection, isostatic uplift, and geomorphological evolution of volcanic islands (Gran Canaria, Canary Islands, Spain). Geomorphology 102, 189–203.

Merritts, D., Vincent, K.R., 1989. Geomorphic response of coastal streams to low, intermediate, and high rates of uplift, Medocino triple junction region, northern California. Geol. Soc. Am. Bull. 101 (11), 1373–1388.

Montgomery, D.R., Foufoula Georgiou, E., 1993. Channel network source representation using digital elevation models. Water Resour. Res. 29 (12), 3925–3934.

Molin, P., Pazzaglia, F.J., Dramis, F., 2004. Geomorphic expression of active tectonics in a rapidly deforming forearc, silca massif, Calabria, southern Italy. Am. J. Sci. 304, 559–589.

Nakata, T., 1989. Active faults of the Himalayas of India and Nepal. Geol. Soc. Am (Special Papers) 232, 243–264.

Necea, D., Fielitz, W., Matenco, L., 2005. Late Pliocene–Quaternary tectonics in the frontal part of the SE Carpathians: insights from tectonic geomorphology. Tectonophysics 410 (1–4), 137–156.

Pathak, V., Pant, C.C., Darmwal, G.S., 2013. Geomorphological and seismological investigations in a part of western Kumaun Himalaya, Uttarakhand, India. Geomorphology 193, 81–90.

Paul, A., 2010. Evaluation and implications of seismic events in garhwal-kumaun region of Himalaya. J. Geol. Soc. India 76 (4), 414–418.

Perron, J.T., Royden, L., 2013. An integral approach to bedrock river profile analysis. Earth Surf. Process. Landforms 38 (6), 570–576.

Phartiyal, B., Kothyari, G.C., 2012. Impact of neotectonics on drainage network evolution reconstructed from morphometric indices: case study from NW India Himalaya. Z. Geomorphol. 56 (1), 121–140.

Ponraj, M., Miura, S., Reddy, C.D., Prajapati, S.K., Amirtharaj, S., Mahajan, S.H., 2010. Estimation of strain distribution using GPS measurements in the Kumaun region of Lesser Himalaya. J. Asian Earth Sci. 39, 658–667.

Quereshy, M.N., Kumar, S., Gupta, G.D., 1989. The Himalaya mega lineament, its geophysical characteristics. Mem. Geol. Soc. India 12, 207–222.

Ray, Y., Srivastava, P., 2010. Widespread aggradation in the mountainous catchment of the Alaknanda–Ganga River System: timescales and implications to Hinterland–foreland relationships. Quat. Sci. Rev. 29 (17–18), 2238–2260.

Rockwell, T.K., Keller, E.A., Johnson, D.L., 1984. Tectonic geomorphology of alluvial fans and mountain fronts near Ventura, California. In: Morisawa, M., Hack, T.J. (Eds.), Tectonic Geomorphology. Publications in Geomorphology, State University of New York, Binghamton, pp. 183–207.

Royden, L., Perron, J.T., 2013. Solutions of the stream power equation and application to the evolution of river longitudinal profiles. J. Geophys. Res. 118, 497–518.

Saklani, P.S., 1993. Geology of the Lower Himalaya (Garhwal). International books and periodicals Delhi, 110034.

Saklani, P.S., Bahuhuna, V.K., 1983. Main Central thrust zone and associated area, Garhwal Himalaya. In: saklani, P.S. (Ed.), Himalayan Shears 1-9. English Book Stores, New Delhi.

Sarkar, I., Jain, R., Khattri, K.N., 2001. Mapping of shallow three dimensional variations of P-wave velocity in Garhwal Himalaya. J. Asian Earth Sci. 19, 155–163.

Sarkar, T., Kannaujiya, S., Taloor, A.K., Ray, P.K.C., Chauhan, P., 2020. Integrated Study of GRACE Data Derived Interannual Groundwater Storage Variability over Water Stressed Indian Regions. Groundwater for Sustainable Development, 100376. https://doi.org/10.1016/j.gsd.2020.100376.

Schumm, S.A., 1956. Evolution of drainage systems and slopes in badlands at Perth Amboy, New Jersey. Geol. Soc. Am. Bull. 67 (5), 597–646.

Schumm, S.A., 1986. Alluvial river response to active tectonics. Active Tectonics 80–94.

Seeber, L., Gornitz, V., 1983. River profile along the Himalayan arc as indicators of active tectonics. Tectonophysics 92, 335–367.

Singh, D.D., Gupta, H.K., 1980. Source dynamics of two great earthquakes of the Indian subcontinent: the Bihar-Nepal earthquake of January 15, 1934 and the Quetta earthquake of May 30, 1935. Bull. Seismol. Soc. Am. 70 (3), 757–773.

Singh, S., Sakalani, P.S., 1978. Some geomorphologic observations in the Ghansyali area. Garhwal Himalaya. Himal. Geol. 8, 813–821.

Singh, A.K., Jasrotia, A.S., Taloor, A.K., Kotlia, B.S., Kumar, V., Roy, S., Ray, P.K.C., Singh, K.K., Singh, A.K., Sharma, A.K., 2017. Estimation of quantitative measures of total water storage variation from GRACE and GLDAS-NOAH satellites using geospatial technology. Quat. Int. 444, 191–200.

Singh, S., Sood, V., Taloor, A.K., Prashar, S., Kaur, R., 2020. Qualitative and quantitative analysis of topographically derived CVA algorithms using MODIS and Landsat-8 data over Western Himalayas, India. Quat. Int. https://doi.org/10.1016/j. quaint.2020.04.048.

Sklar, L., Dietrich, W.E., 1998. River longitudinal profiles and bedrock incision models: stream power and the influence of sediment supply. Geophys. Monograph American Geophys. Union 107, 237–260.

Snyder, N.P., Whipple, K.X., Tucker, G.E., Merritts, D.J., 2000. Landscape response to tectonic forcing: digital elevation model analysis of stream profiles in the Mendocino triple junction region, northern California. Geol. Soc. Am. Bull. 112 (8), 1250–1263.

Sood, V., Gusain, H.S., Gupta, S., Taloor, A.K., Singh, S., 2020. Detection of snow/ice cover changes using subpixel-based change detection approach over Chhota-Shigri glacier, Western Himalaya, India. Quat. Int. https://doi.org/10.1016/j. quaint.2020.05.016.

Srivastava, P., Mitra, G., 1994. Thrust geometries and deep structure of the outer and lesser Himalaya, Kumaon and Garhwal (India): implications for evolution of the Himalayan fold-and-thrust belt. Tectonics 13 (1), 89–109. https://doi.org/10.1029/ 93TC01130.

Strahler, A.N., 1952. Hypsometric (area-altitude) analysis of erosional topography. Geol. Soc. Am. Bull. 63 (11), 1117–1142.

Taloor, A.K., Ray, P.K.C., Jasrotia, A.S., Kotlia, B.S., Alam, A., Kumar, S.G., Kumar, R., Kumar, V., Roy, S., 2017. Active tectonic deformation along reactivated faults in Binta basin in Kumaun Himalaya of north India: inferences from tectono-geomorphic evaluation. Z. Geomorphol. 61 (2), 159–180.

Taloor, A.K., Kotlia, B.S., Jasrotia, A.S., Kumar, A., Alam, A., Ali, S., Kouser, B., Garg, P. K., Kumar, R., Singh, A.K., Singh, B., 2019. Tectono-climatic influence on landscape changes in the glaciated Durung Drung basin, Zanskar Himalaya, India: a geospatial approach. Quat. Int. 507, 262–273.

Taloor, A.K., Pir, R.A., Adimalla, N., Ali, S., Manhas, D.S., Roy, S., Singh, A.K., 2020. Spring water quality and discharge assessment in the Basantar watershed of Jammu Himalaya using geographic information system (GIS) and water quality Index (WQI). Groundwater Sustain. Develop. https://doi.org/10.1016/j.gsd.2020.100364.

Talukdar, R., Kothyari, G.C., Pant, C.C., 2019. Evaluation of neotectonic variability along major Himalayan thrusts within the Kali River basin using geomorphic markers, Central Kumaun Himalaya, India. Geol. J. https://doi.org/10.1002/gj.3452.

Tapponnier, P., Molnar, P., 1977. Active faulting and tectonics in China. J. Geophys. Res. 82, 2905–2930.

Thakur, V.C., 2004. Active tectonics of Himalayan frontal thrust and seismic hazard to Ganga Plain. Curr. Sci. 86, 1554–1560.

Tucker, G.E.R., Slingerland, R., 1997. Drainage basin responses to climate change. Water Resour. Res. 33 (8), 2031–2047.

Valdiya, K.S., 1980. Geology of Kumaun Lesser Himalaya. Wadia Institute of Himalayan Geology, Dehradun, pp. 1–291.

Valdiya, K.S., 1981. Tectonics of the central sector of the Himalaya. In: Gupta, H.K., Delany, F.M. (Eds.), Zagros, Hindu Kush, Himalaya: Dynamic Evolution. American Geophysical Union Geodynamics Series3, pp. 87–110.

Valdiya, K.S., 1993. Uplift and geomorphic rejuvenation of the Himalaya in the Quaternary period in the Quaternary history of India. Curr. Sci. 64, 873–885.

Valdiya, K.S., 1999. Reactivation of faults, active folds and geomorphic rejuvenation in eastern Kumaun Himalaya: wider implication. Indian J. Geol. 1–2, 53–63. Valdiya, K.S., Kotlia, B.S., Pant, P.D., Shah, M., Mungali, N., Tewari, S., Sah, N., Upreti, M., 1996. Quaternary palaeolakes in Kumaun Lesser Himalaya: finds of neotectonic and palaeoclimatic significance. Curr. Sci. 70, 157–160.

Waikar, M.L., Nilawar, A.P., 2014. Morphometric analysis of a drainage basin using geographical information system: a case study. Int. J. Med. Clin. Res. 2, 179–184.

Wallace, R.E., Moxham, R.M., 1967. Use of infrared imagery in study of the San Andreas fault system, California. Geol. Survey Res. 575, 147.

Weissel, J.K., Seidl, M.A., 1998. Inland Propagation of Erosional Escarpments and River Profile Evolution across the Southeast Australian Passive Continental Margin. Rivers over Rock: Fluvial Processes in Bedrock Channels, pp. 189–206.

Whipple, K.X., Di-Biase, R.A., Crosby, B.T., 2013. Bedrock rivers. Treatise on Geomorphol. 9, 550–570.

Whittaker, A.C., 2007. Investigating controls on bedrock river incision using natural and laboratory experiments. Phd thesis. http://hdl.handle.net/1842/14662.

Wobus, C.W., Whipple, K.X., Hodges, K.V., 2006. Neotectonics of the central Nepalese Himalaya: constraints from geomorphology detrital 40Ar/39Ar thermochronology and thermal modeling. Tectonics 25 (TC4011). https://doi.org/10.1029/ 2005TC001935.

Xue, L., Alemu, T., Gani, N.D., Abdelsalam, M.G., 2018. Spatial and temporal variation of tectonic uplift in the southeastern Ethiopian Plateau from morphotectonic analysis. Geomorphology 309, 98–111.

Yeats, R.S., Thakur, V.C., 2008. Active faulting south of the Himalayan Front: establishing a new plate boundary. Tectonophysics 453, 63–73.

Yin, A., 2006. Cenozoic tectonic evolution of the Himalayan orogen as constrained by along-strike variation of structural geometry, exhumation history, and foreland sedimentation. Earth Sci. Rev. 76, 1–131.

Yin, A., Harrison, T.M., 2000. Geological evolution of the himalayan Tibetan orogen. Annu. Rev. Earth Planet Sci. 28, 211–280.